12-2009

SIAA and Neat2 Heme Binding Proteins from Streptococcus Pyogenes

Giselle M. Delgado
Georgia State University, gdelgado1@student.gsu.edu

SIAA AND NEAT2 HEME BINDING PROTEINS FROM *STREPTOCOCCUS PYOGENES*

by

GISELLE M. DELGADO

Under the direction of Dabney W. Dixon

ABSTRACT

The bacterium *Streptococcus pyogenes* requires heme, which is taken up via an ABC transporter. An understanding of this pathway may result in new approaches to antibacterial agents. Both SiaA and NEAT2 (NEAr Transporter 2) are proteins involved in heme binding. One of the axial ligands of SiaA, His 229, was purified to study how mutagenesis affects heme binding. UV-visible studies showed a small band at 420 nm with respect to the protein band at 288 nm which probably indicates that heme was lost easily from this mutant. We have also worked to optimize the yield of Shr-NEAT2 by changing different variables. For each of the batches, the yield of holoNEAT2 was calculated by UV-visible spectroscopy. Increasing oxygen during growth did not improve holoNEAT2 yield. On the other hand, lower temperature, decrease in time after induction, and addition of ALA all increased the protein production.

INDEX WORDS: SiaA, NEAT domain, ABC transporters, Heme, *Streptococcus pyogenes*

SIAA AND NEAT2 HEME BINDING PROTEINS FROM *STREPTOCOCCUS PYOGENES*

by

GISELLE M. DELGADO

A Thesis Submitted in Partial Fulfillment of the Requirements of the Degree of

Master of Science

in the College of Arts and Sciences

Georgia State University

2009

SIAA AND NEAT2 HEME BINDING PROTEINS FROM *STREPTOCOCCUS PYOGENES*

by

GISELLE M. DELGADO

Committee Chair: Dabney W. Dixon

Committee: Kathy Grant

Zehava Eichenbaum

Electronic Version

Offices of Graduate Studies

College of Arts and Sciences

Georgia State University

December 2009

ACKNOWLEDGEMENTS

I would like to thank God for giving me the strength and faith to achieve my goals in life.

I would like to thank the Department of Chemistry at Georgia State University for accepting me into the program and to Dr. Dabney Dixon for believing in my talent and for her guidance to be a better person. Dr. Grant and Dr. Eichenbaum, thank you for being part of my committee and for helping me be a successful student. I want to thank Dr. Dixon's lab group for helping me during my career and sharing with me great moments that I will never forget. I also want to thank my family, especially my mom and my two brothers, Hector and Edgardo, for the support they have always given me. Last but not least, I want to thank my fiancé Michael for being my partner in life and success and his family for being there when I needed them the most.

TABLE OF CONTENTS

LIST OF TABLES

LIST OF FIGURES

CHAPTER 1

LIST OF ABBREVIATIONS

ABC transporters: ATP-Binding Cassette (ABC) transporters

AHT: anhydrotetracycline

AMP: ampicillin

APS: ammonium persulfate

δ-ALA: delta aminolevulinic acid

Hp: Haptoglobin

MCD: magnetic circular dichroism

MetHb: methemoglobin

NEAT: NEAr Transporter

NMR: nuclear magnetic resonace

PBPs: periplasmic binding proteins

rR: resonance Raman

SDS-PAGE: sodium dodecyl sulfate polyacrylamide gel electrophoresis

UV-vis spectroscopy: ultraviolet visible spectroscopy

WT: wild type

CHAPTER 1. SIAA, A HEME BINDING PROTEIN

1.1. Overview of *S. pyogenes*, a pathogenic bacterium.

S. pyogenes, also known as Group A streptococcus (GAS) and the "flesh eating bacterium," is a gram positive pathogen which targets the throat and skin. Common diseases of this bacterium are pharyngitis, impetigo, scarlet fever, toxic shock syndrome, and post streptococcal infections which include rheumatic fever (Cunningham, 2000).

Antibiotic resistance of common pathogens is a growing clinical issue (Kumar & Schweizer, 2005; Poole, 2007; Li & Nikaido, 2009; Martinez et al., 2009) making the development of new antibiotics a high priority. One strategy for the development of novel antibiotics is to target a pathway found in bacteria, but not in humans. Because humans make their own heme (Dailey, 1997; Heinemann et al., 2008). The heme uptake pathway is an excellent target for those bacteria which do not have the genetic machinery to produce their own heme. *S. pyogenes* is such a bacterium, and therefore its heme uptake pathway is an excellent pharmaceutical design target (Skaar & Schneewind, 2004).

Many pathogenic bacteria can use heme to acquire iron needed for their survival (Wandersman & Delepelaire, 2004; Crosa et al., 2004; Wilks & Burkhard, 2007; Cavallaro et al., 2008; Krewulak & Vogel, 2008; Tong & Guo, 2009). Heme accounts for approximately 75% of iron in humans (Grigg et al., 2007b). Pathogens have developed mechanisms to acquire iron from heme (Wilks & Burkhard, 2007; Cavallaro et al., 2008). The systems in which heme is used have been related to virulence and infections (Wilks & Burkhard, 2007; Grigg et al., 2007b).

Cavallero et al. have analyzed 437 genomes known to be related to heme biosynthesis and uptake in bacteria (Cavallaro et al., 2008). Of these, 138 can synthesize heme, 20 can obtain heme from an external source, 218 can do both and 61 can do neither. Thus, 86% of bacteria

analyzed can synthesize heme, acquire heme, or both. *S. pyogenes* can acquire heme from its environment, taking it from hemoglobin, myoglobin, heme-albumin, catalase and the hemoglobin/haptoglobin complex (Francis, Jr. et al., 1985; Eichenbaum et al., 1996).

1.2 ABC Transporters.

Bacteria use different transport systems to acquire iron (in the case of *S. pyogenes*, an ATP-Binding Cassette (ABC) transporter is used shown in Figure 1). ABC transporters are membrane proteins that use ATP hydrolysis to transport molecules across membranes (Jones & George, 2004; Davidson & Maloney, 2007; Hollenstein et al., 2007). They are classified as primary active transporters meaning that movement of molecules occurs against a gradient, requiring energy. These transporters are found in prokaryotes and eukaryotes and take part in processes such as homeostasis, bacterial immunity, and uptake of molecules by pathogenic bacteria.

ABC transporters move molecules in one direction through the membrane. They are classified as importers and exporters. Importers are found in prokaryotes, and need a binding protein to deliver molecules to the transporter. Exporters are found in prokaryotes and eukaryotes and do not need a binding protein; they obtain the molecules to be transported directly from the cytoplasm.

ABC transporters are made of two transmembrane domains (TMD) and two nucleotide-binding domains (NBDs). The TMDs vary in length, primary sequence, and number of transmembrane helices. TMDs are formed of hydrophobic segments which form channels needed for the transport of molecules.

NBDs have a conserved three-dimensional structure. NBDs are hydrophilic molecules and undergo conformational changes promoted by the hydrolysis of ATP. NBDs are divided into

subparts including the Walker A and B motifs, LSGGQ motif, Q-loop, D-loop, and A-loop. The C- loop allows interaction of the ATP γ-phosphate from the other subunit of the dimer. The D-loop is involved in the interactions of the two NBDs. The Q-loop is involved in the NBD-TMD contact. The A-loop is part of the catalytic reaction.

The conformational changes in NBDs are transferred to the TMDs through non-covalent interactions. There are several motifs involved with NBDs which provide for the binding of ATP, place correct amino acids in appropriate position for hydrolysis, and contact with TMDs and NBDs.

The HI1470/1 transporter from *Haemophilus influenzae* and the BtuCD (cobalamin) transporter from *E. coli* have side by side interaction of TMDs (Davidson & Maloney, 2007). However, the translocation pathways are different. In the HI1470/1 transporter, the translocation pathway is open to the cytoplasm and access from the periplasmic side is restricted by residues in the TM helices. In BtuCD, the translocation pathway is open to the periplasm and access to the cytoplasm is restricted by residues in the TM helices.

The ABC transporter that takes up heme in *S. pyogenes* is termed SiaA (Bates et al., 2003) and alternatively HtsA (heme transport) (Liu & Lei, 2005). SiaA (spy 1795) is part of a 10 gene cluster (Figure 1); SiaB (spy 1794) and SiaC (spy 1793) are immediately downstream. Upstream are two additional proteins in the cluster, Shr and Shp. It is now known that heme is transferred from Shr to Shp to SiaA (Lei et al., 2002; Lei et al., 2003; Liu & Lei, 2005; Nygaard et al., 2006) In this chapter, we outline information related to SiaA and Shp; background information relevant to Shr is given in Chapter 2.

Shp is a heme binding protein found in *S. pyogenes* cell surface (Zhu et al., 2008b). UV-visible spectroscopy studies show that heme is transferred from hemoglobin to apo-Shp, forming

holo-Shp. Holo-Shp has a six-coordinate heme center and shows abosrption peaks at 428, 528, and 560 nm (Nygaard et al., 2006). UV-visible spectroscopy studies show that Shp transfers heme to SiaA but that SiaA does not transfer heme back to Shp. The crystal structure of Shp shows that heme binds with two methionine residues, Met153 and Met66 (Aranda et al., 2007).

SiaA is a 37 kDa heme binding lipoprotein. MCD (magnetic circular dichroism), NMR (nuclear magnetic resonance), and rR (resonance Raman) studies demonstrated that this protein has a six coordinate heme center (Sook et al., 2008). Holo-SiaA has an absorption peak at 412 nm (Liu & Lei, 2005). Protein denaturation with guanidinium showed that the ferric state of the protein is less stable than the ferrous state (Sook et al., 2008). SiaA has two axial ligands, His229 and Met79 (Figure 2). The mutation of these two residues to alanines showed a decrease in the intensity of the Soret band.

1.3 SiaA homologs.

SiaA homologs are found in both Gram positive and Gram negative bacteria. Because the first chapter of this thesis focuses on SiaA, we describe here literature studies on known homologs including IsdE (SiaA threaded into IsdE shown in Figure 3) from the Gram positive bacteria *Staphylococcus aureus* as well as ShuT, PhuT, ChuX and HmuY from Gram negative bacteria.

1.3.1 IsdE.

IsdE is a 33 kDa heme binding lipoprotein found in *Staphylococcus aureus* (Grigg et al., 2007a). This protein contains a long α- helix. IsdE contains two domains that have beta-sheets surrounded by α-helices. In the C-terminal domain there are 5-stranded β-sheet and in the N-terminal domain there are a total of two β-strands.

IsdE contains a 6-coordinate heme center. IsdE showed a strong Soret band at 400 nm (Grigg et al., 2007a). In early work, the mutation of each His229 and Met78 to alanine individually showed reduction of heme binding in UV-visible spectra. The mutation of His229 and Met78 together showed higher reduction of heme binding than each mutant individually. This data suggested that both His229 and Met78 were probable axial ligands. The H229A spectrum was found to be different from the WT IsdE in the MCD spectrum. WT IsdE showed a band at 568 nm in the MCD spectrum but H229A showed a band at 590 nm (Pluym et al., 2007). The crystal structure of IsdE shows that besides participating as an axial ligand, His229 is involved in hydrogen bonding in the heme binding pocket. One of the hydrogen bonds that it forms is with Glu265 (Grigg et al., 2007a).

1.3.2 PhuT.

PhuT is a 33 kDa heme binding protein found in *Pseudomonas aeruginosa* (Tong & Guo, 2007). PhuT contains a five-coordinate ferric heme center. The protein is comprised of 24-26% α- helices, 20-21% of β-sheets, 19-22% of turns and 28-37% of other structures (Tong & Guo, 2007).

PhuT showed a broad Soret band at 400 nm. Besides this band, PhuT showed bands at 500, 534, and 624 nm. Addition of a reducing agent, dithionite, produced a redshift of the 400, 500 and 534 nm bands to 420, 560 and 589 nm, respectively.

A recent X-ray study has shown that Tyr71 is the axial ligand of PhuT (Tong & Guo, 2007). The WT PhuT as well as the Y71F and Y146F mutants were studied. Y146 was not proposed as a possible axial ligand, but it was mutated to F in order to compare the results with Y71F. The Y146F PhuT mutant showed a UV-visible spectrum similar to WT PhuT. However, Y71 showed a different spectrum, consistent with the role of this residue as the axial ligand.

1.3.3 ShuT.

ShuT is a 28.3 kDa heme binding protein found in *Shigella dysenteriae* (Eakanunkul et al., 2005). ShuT contains a five-coordinate ferric heme center. Wild type ShuT showed a Soret band at 400 nm. Other bands were detected at 500, 521, and 617 nm. In early work, Y94A, Y228F, and Y228F /Y94A spectra were compared to determine the probable axial ligand of ShuT (Eakanunkul et al., 2005). The spectrum of the Y228/Y94A and Y94A mutants were similar to one another and different from WT ShuT. The spectra similarity between WT ShuT and Y288F indicated that Y228 was probably not an axial ligand (Eakanunkul et al., 2005). Thus, it was concluded that Y94 was the probable axial ligand.

The crystal structure of ShuT indicated that Tyr94 is the heme axial ligand. This was also indicated by resonance Raman spectroscopy and magnetic circular dichroism spectroscopy. In the resonance Raman spectrum, WT ShuT and Y228F ShuT mutant showed similar or identical bands. Likewise, Y94A and Y228F/Y94A showed similar or identical bands in the spectrum. For example, the ν_{10} band for WT ShuT and Y228F ShuT mutant was at around 1616 cm^{-1}. For Y94A and Y228F/Y94A, the ν_{10} band was at 1625 cm^{-1}. The MCD spectra results corresponded with the resonance Raman results. The spectra for WT ShuT and Y228F ShuT mutant were found to be almost the same. The spectra of Y94A and Y288F/Y94A were also found to be very similar to each other. Both resonance Raman spectroscopy and MCD indicated that Tyr94 was the axial ligand of ShuT. MCD did not show the presence of a histidine ligand.

1.3.4 ChuX. ChuX is a heme binding protein found in *E. coli* (Suits et al., 2009). This protein is a homodimer, each half of which binds two hemes. Spectral studies show that the ferric ChuX has a combination of 5-coordinate high spin and 6-coordinate low and high spins. Ferrous ChuX

has a combination of 5-coordinate high spin and 6-coordinate low spin states. This protein has two axial ligands, His65 and His98.

1.3.5 HmuY. HmuY is a heme binding lipoprotein from the bacterium *Porphyromonas gingivalis* (Olczak, 2006; Olczak et al., 2008). HmuY is found as a monomer but can also form dimers and oligomers. This protein binds heme as shown by UV-visible spectroscopy studies mixing hemin with apo-HmuY. HmuY has two axial ligands, His134 and His166 (Wojtowicz et al., 2009c; Wojtowicz et al., 2009a; Wojtowicz et al., 2009b). The crystal structure of this protein shows a tetrameric quaternary structure and iron has an octahedral coordination.

1.4 Experimental

LB medium preparation. A batch of LB medium was made by adding 15 g tryptone, 7.5 g Bacto^{TM} yeast extract, 15 g NaCl, and 1500 mL water to a 2.8 L Erlenmeyer flask. The pH was adjusted to 7.01 by addition of aqueous NaOH. The solution was autoclaved using the liquid cycle for 15 min and cooled to room temperature. A total of 1.5 mL AMP stock solution was added to the LB medium. LB medium (30 mL) was added to a 125 mL Erlenmeyer flask.

Inoculation of LB medium and growth of H229A transfected *E. coli*. Under sterile conditions, Top10ShuA-His [a gift from Dr. Eichenbaum (Georgia State University)] was added with an inoculating loop to the 50 mL solution in the 125 mL Erlenmeyer flask. The solution was shaken for a period of 16 h at 37°C, at which point OD_{660} was about 1. The remaining LB solution (~1450 mL at room temperature) was mixed with new inoculated solution and shaken for 3 h at 37°C to a final OD_{660} of 0.5. A 2% arabinose stock solution [a gift from Kyle Chan (Georgia State University)] was prepared by dissolving 4 g L-arabinose (Acros Organics, New Jersey) in 200 mL sterile water. A total of 7.5 mL of 2% arabinose stock solution was added to the flask. The flask was incubated for 4 h at 37°C. The culture broth was evenly distributed into

1 L sterile plastic centrifuge bottles and centrifuged at 8000 x g for 20 min at 4°C. The supernatant was discarded; the pellet was scraped into a sterile vial and the sample stored in the -80°C freezer.

French press sample preparation and pressing. The centrifuge bottles containing the cell pellet were removed from the -80 °C freezer and quickly thawed using warm water. The cell pellets were transferred from the centrifuge bottles to a 50 mL Falcon tube using an inoculating loop. Approximately, 40 mL of lysis buffer (1 L lysis buffer: 20 mL of 1 M Tris HCl, pH 8.0 from 20 mM Tris base, 100 mM NaCl, 1 mL of 0.1% Triton X-100 (Fisher Scientific), and 100 mL 10% glycerol) [(a gift from Joy Zhou (Georgia State University)] was added to a 50 mL Falcon tube. A total of 4 protease inhibitor tablets (Complete Mini, EDTA-free, Roche Diagnostics, Mannheim, Germany) was added and dissolved. The solution then was divided into two Falcon tubes, each with approximately the same amount of solution. The solutions were placed on ice and kept on ice while not being actively French pressed. A SimAminco French pressure cell press was used on high setting and adjusted to a display psi of 1280. Ethanol was sprayed in the plunger to make insertion easier. A large Thermo French press cell (35 mL maximum volume), kept at 4 ºC, was loaded with one sample (~20 mL). The sample was released by slowly tapping on the T-screw and putting it in its original Falcon tube in the ice bucket. After the sample was collected, the selector was set to down and the sample remaining was stored also in the Falcon tube. Each solution was French pressed twice. The pressure was decreased to 0 psi and the French press machine was turned off. The French press equipment was cleaned with water and ethanol and air dried before it was stored in the refrigerator. The samples in the Falcon tubes were centrifuged at 15,000 × g for 20 min at 4 ºC. The supernatant was

decanted and the solution was filtered using syringe and a Nalgene disposable bottle top filter 150 mL 0.45 μm pore size (Fisher Scientific).

SDS-PAGE gel preparation (sodium dodecyl sulfate polyacrylamide gel electrophoresis) Resolving and stacking gel solutions were made to prepare two 0.75 mm SDS-PAGE gels. The resolving gel solution was made by adding 2.3 mL water, 5.0 mL 30% acrylamide (made by adding 30 g of acrylamide/bis (EM Science, Gibbstown, NJ) and 100 mL water), 2.5 mL 1.5 M Tris pH 8.8 (made by dissolving 36.34 g Tris (FisherBiotech, Fair Lawn, NJ) in water to make a 200 mL stock solution), 100 μL 10% SDS (sodium dodecyl sulfate) (made by mixing 1 g SDS with 10 mL water), 100 μL 10% APS (ammonium persulfate) (made by mixing 1 g AMP sodium salt (FisherBiotech) with 10 mL of sterile water), and 4 μL TEMED (tetramethylethylenediamine) (Bio-Rad Lab) into an autoclaved Erlenmeyer flask. The stacking gel solution was made by adding 6.8 mL water, 1.7 mL 30% acrylamide, 1.25 mL 1.0 M Tris pH 6.8 (made by dissolving ~25 g Tris in water to make a 200 mL stock solution), 10% SDS, 100 μL 10% APS, and 10 μL TEMED into an autoclaved Erlenmeyer flask. The resolving gel was poured first, 2-propanol was added, and the gel was dried for ~ 40 min. Water was used to rinse the gel; filter paper was used to remove excess water, and the stacking gel was added and dried for ~ 40 min.

SDS-PAGE gel run. A running buffer solution was made by adding 50 mL Tris-glycine-SDS 10X (Fisher Scientific) and 450 mL water in a volumetric flask and was inverted five times. The Mini-PROTEAN 3 cell equipment was set up as outlined in the manual using 0.75 mm plates. The running buffer was added to the Mini-PROTEAN 3 cell equipment. A sample buffer was made by adding 25 μL of 2-mercaptoethanol (Bio-Rad Lab) and 475 μL of Laemmli sample buffer (Bio-Rad Lab) into an Eppendorf tube. The Laemmli sample buffer provided the dye for

the protein. A total of 20 µL of sample buffer and 10 µL of the protein (NEAT2) were mixed in an Eppendorf tube, centrifuged in the VWR Mini Centrifuge C-1200 at 6,000 × g for 30 s, and heated for 5 min in the heat block at 103 ºC. The Precision Plus All Blue Standards protein ladder (5 µL) (Bio-Rad Lab) and the sample buffer plus protein (10 µL) were loaded into different wells. The electrophoresis system was initially set to 70 V. When the dye front was approximately 1 cm below the bottom of the well, the system was switched to 118 V. The sample was run until the dye front reached the bottom of the SDS-PAGE gel. Destaining solution was prepared by adding 500 mL of methanol (Caledon, Georgetown, Canada) to 400 mL of water and 100 mL glacial acetic acid (EMD, Gibbstown, NJ). Staining solution was prepared by adding 0.5 g Coomassie Brilliant Blue R-250 (Bio-Rad Lab) to 200 mL of destaining solution. The gel was washed with water and placed in staining solution for 30 min. The gel was placed in destaining solution for 1 h and 30 min. The gel was dried using the DryEase Mini-Gel Drying System (Invitrogen, Carlsbad, CA).

Nickel affinity FPLC followed the published protocol (Sook et al., 2008).

UV- visible spectroscopy. A Cary 50 Bio UV-visible spectrophotometer was used for all the absorbance determinations. To each 100 µL of protein, 300 µL of 20 mM Tris-Cl 10% glycerol buffer (recipe) were added in a 6Q cuvette. The base line was recorded with the blank sample that contained the buffer 20 mM Tris-Cl 10% glycerol. The range used to record the spectrum was 700 – 250 nm.

Western blotting. The equipment for Western blotting (Bio-Rad) was prepared by soaking two fiber pads in transfer buffer [a gift from Tanu Soni (Georgia State University)]. A PVDF (polyvinylidene fluoride) membrane with filter paper (a gift from Tanu Soni) was used for the blotting and was soaked in transfer buffer. The gel sandwich cassette was set up with the black

side down on a clean surface. A pre-wetted fiber pad was placed on the black side of the cassette, followed by a piece of filter paper, the SDS-PAGE gel, the pre-wetted membrane, a piece of filter paper on top of the membrane, and the last fiber pad. A glass tube was used to remove any air bubbles found on the membrane. The cassette was placed in the module and the frozen Bio-Ice cooling unit was placed on one of the sides of the cassette. The apparatus was set to 70 V and was run for 1 h. A TBST (Tris-Buffered Saline Tween) (20 mL Tris HCl adjusted to pH 7.5, 30 mL of 5 M NaCl, and 950 mL water for a total of 3 L and Tween (Invitrogen, Carlsbad, CA) added to a 0.05% concentration solution) (a gift from Tanu Soni) was added to the protein side of the membrane and rotated for 5 min twice. A blocking solution was prepared by mixing 1.5 g of skim milk and 25 ml of TBST. The blocking solution was placed on the membrane for one hour after the TBST was discarded. The anti-SiaA antibody (a gift from Dr. Eichenbaum) solution was prepared by adding 1 μL of anti-SiaA antibody to the blocking solution. The anti-SiaA antibody was placed on the membrane and rotated for 1 h. The anti-SiaA antibody solution was poured out and the membrane washed with TBST for 5 min three times. A total of 2.5 μL of anti-rabbit antibody solution (a gift from Dr. Eichenbaum) was added to 25 mL of blocking solution and poured in the membrane for one hour. The membrane was washed with TBST three times and once with TBS. The substrate was prepared by adding one ready to use tablet of BCIP + NBT (Roche Applied Science, Indianapolis, IN) with 10 mL of Tris HCl and $MgCl_2$. The substrate was added to the membrane and placed in a dark place for approximately 8 min until color developed. Water was used to stop the color development.

Homology modeling using LOOPP (Learning, Observing and Outputting Protein Patterns) (Teodorescu et al., 2004) and Rasmol (Sayle & Milner-White, 1995) The wild type SiaA protein sequence was threaded using LOOPP, (http://cbsuapps.tc.cornell.edu/loopp.aspx). First,

the sequence was pasted in the “input sequence” section. A total of 5 homologous sequences were obtained and three were chosen based on percent similarity: BtuF (1N2Z_A), CeuE (2CHU_A), and FhuD (1K7S_N). The chosen structures were visualized using Rasmol.

BLAST (Basic Local Alignment Search Tool). The PhuT, ShuT, and IsdE protein sequences were analyzed using BLAST (http://blast.ncbi.nlm.nih.gov/Blast.cgi)(Altschul et al., 1997). First, the FASTA sequence was pasted into the protein-blast program. The algorithm selected was blastp (protein-protein BLAST). Several homolog sequences were obtained but only the most similar were analyzed.

1.5 Results and Discussion

1.5.1 Homology Modeling and BLAST

The text above summarizes the X-ray structures of PhuT, ShuT, and IsdE. In early work (before the X-ray structures were known), we performed homology modeling of these proteins. This section will outline those studies. Also, in early work we performed homology modeling of SiaA with proteins that had known crystal structures. The work is not described in the text but can be seen in Figure 4.

1.5.1.1 PhuT.

PhuT was analyzed with BLAST and several homolog sequences were obtained. The sequences that were examined for identities, positives (similarities), and gaps were those of CeuE in a complex with the iron binding mecam, BtuF: the vitamin B_{12} binding protein of *E. coli*, and FhuD complexed with gallichrome. The identities, positives, and gaps percentages were found to be very similar for CeuE (23%, 44%, and 6%, respectively), BtuF (25%, 44%, and 5%, respectively) and FhuD showed (23%, 37%, and 6%, respectively).

PhuT was threaded into three homologs: CeuE (2CHU_A); BtuF (1N4A_A); and FhuD (1EFD_N). The amino acids around the heme binding pocket were examined and compared with the heme binding pocket of PhuT.

The heme binding pocket of PhuT showed one axial ligand, Tyr71. The structures of CeuE, BtuF, and FhuD showed Tyr71 in the heme binding pocket. The three homologs showed Try71 in a similar position as Tyr71 in PhuT.

The heme binding pocket of PhuT also showed the charged residues, Arg73 and Arg228. These positively charged amino acids can interact with the two heme-propionates. PhuT showed other charged amino acids such as His and Lys but there are not located on the heme binding pocket. CeuE and BtuF illustrated Arg73 and Arg228 on the heme binding pocket. The side chains of Arg73 and Arg228 in CeuE and BtuF point to the center of the pocket. FhuD has three Arg in the pocket the pocket, Arg73, Arg236, and Arg228. The Arg residues point to its center. Arg was the only charged amino acid that seems to interact in the pocket. The other charged amino acids such as His and Lys are not close to the pocket or are not well positioned to bind with other molecules.

1.5.1.2 ShuT.

ShuT was analyzed with a BLAST search and several homolog sequences were obtained. The identities, positives, and gap percentages were found to be very similar for CeuE (23%, 44%, and 7%, respectively) and BtuF (28%, 51%, and 4%, respectively).

ShuT was threaded into three homologs CeuE (2CHU_A); BtuF (1N4A_A); and FhuD (1EFD_N). The amino acids around the heme binding pocket were examined.

The heme binding pocket of ShuT showed one axial ligand, Tyr 94. The structures of CeuE, BtuF, and FhuD showed Tyr94 on the heme binding pocket. The three homologs showed Tyr94 in a similar position as ShuT.

The heme binding pocket also showed charged residues. CeuE showed Lys122 and Arg164 on the heme binding pocket. Lys122 and Arg164 were not located close to each other. FhuD showed Lys122 and Arg164 on the pocket. The side chains of Lys122 and Arg164 pointed towards the middle of the pocket. Lys122 and Arg164 were located on the same side of the heme binding pocket. BtuF showed Lys116 and Arg185 on the pocket. The side chains of Lys116 and Arg185 pointed towards the heme binding pocket. BtuF showed two His close to the heme binding pocket but the immidizole rings point away from the pocket. Lys and Arg were the only positively charged amino acids that seemed to interact in the heme binding pocket.

1.5.1.3 IsdE. IsdE was threaded into four homologs CeuE (2CHU_A); BtuF (1N4A_A); FhuD (1EFD_N); and FeuA from *Bacillus subtilis* (2PHZ_A). The amino acids around the heme binding pocket were examined.

The heme binding pocket of IsdE showed two axial ligands, His229 and Met78. The structures of CeuE, BtuF, FhuD, and FeuA showed both His229 and Met78 in the heme binding pocket. For all the structures, His229 and Met78 were located in opposite sides of the pocket. The only difference was that the structure of BtuF showed both axial ligand farther apart than His229 and Met78 in CeuE, FhuD, and FeuA.

The heme binding pocket also showed charged residues. IsdE showed Lys62 and Arg206 in the heme binding pocket. The side chains of Lys62 and Arg206 pointed towards the center of the heme binding pocket. Both side chains pointed in opposite directions. CeuE showed Lys62 on the heme binding pocket. Lys62 was located on the opposite side of His229, closer to Met78.

Lys62 side chain points towards the center of the pocket. BtuF showed Lys62 and Lys237 on the heme binding pocket. Arg206 and Arg226 are on the heme binding pocket also. Arg206 seemed to be in a better position to bind than Arg226. FeuA showed Arg206 and Lys62 in the heme binding pocket. Arg206 and Lys62 were located in opposite sides of the pocket. Both amino acids pointed in the same direction. However, Lys62 was closer to Met78 and Arg206 was closer to His229. Lys and Arg seemed to be the only positively charged amino acids on the heme binding pocket.

1.5.2 Expression and Purification of H229A

The expression of H229A was confirmed by a band at 37 kDa shown in the Western Blot in Figure 5. The isolation of H229A from other proteins was achieved by FPLC (Figure 6) using a nickel column affinity described by the method above. The SDS-PAGE in Figure 6 shows a single band at 37 kD. The spectrum for H229A (Figure 7) shows that the Soret band is approximately 5-10% the band at 280 nm.

1.6. Conclusion

Expression and purification of H229A was achieved as shown by the SDS-PAGE and Western Blot. Figure 7 shows the UV-visible spectrum of H229A. The low Soret band indicates that histidine (one of the axial ligands of SiaA) to alanine, results in substantial heme loss. The Soret band is only around 10% of the protein band at 280 nm. These data are consistent with H229 as an axial ligand for the heme.

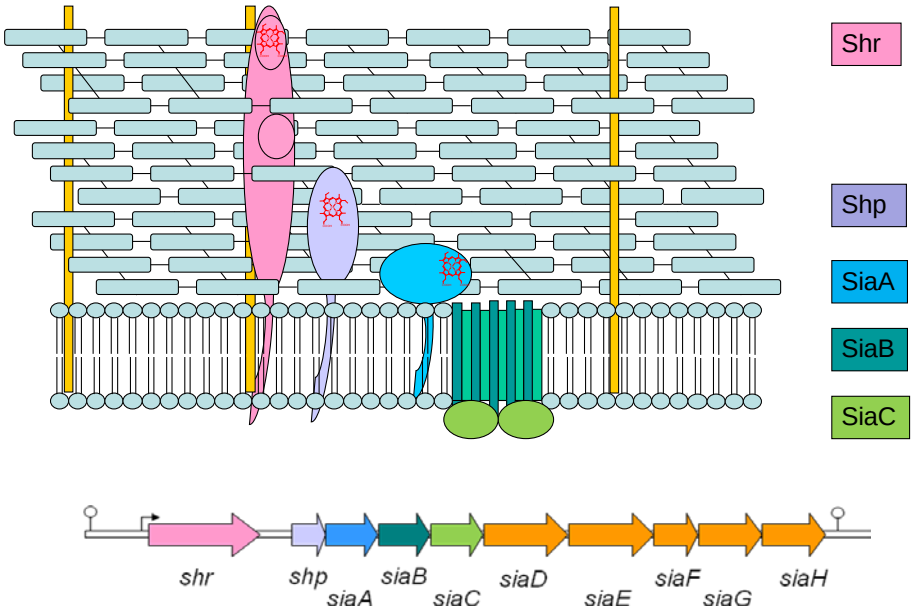

Figure 1. ATP binding cassette (ABC) transport system: SiaABC and schematic diagram of the SiaA/Hts Gene Cluster.

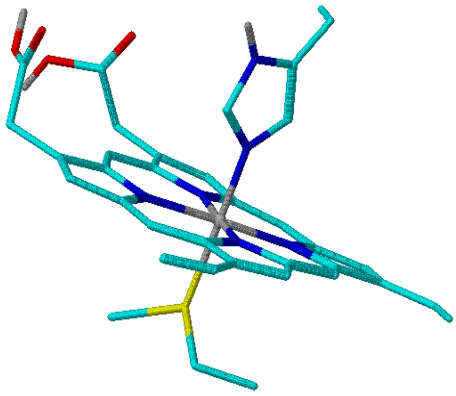

Figure 2. A model of the His and Met axial ligands of SiaA. Histidine and methionine bind heme in SiaA from opposite sides.

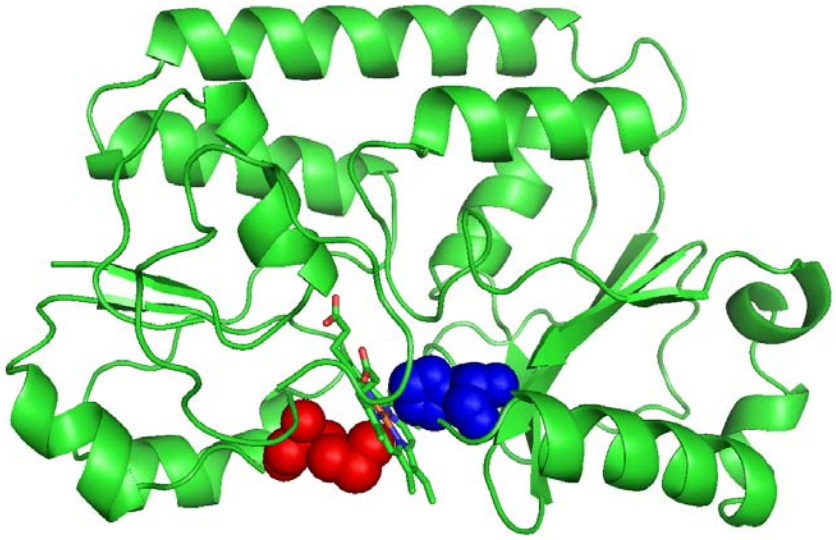

Figure 3. SiaA threaded into IsdE (2Q8Q.pdb) (Grigg et al., 2007a). The axial ligands are shown in red (Met79) and blue (His229). This structure was visualized using Pymol (DeLano, 2009).

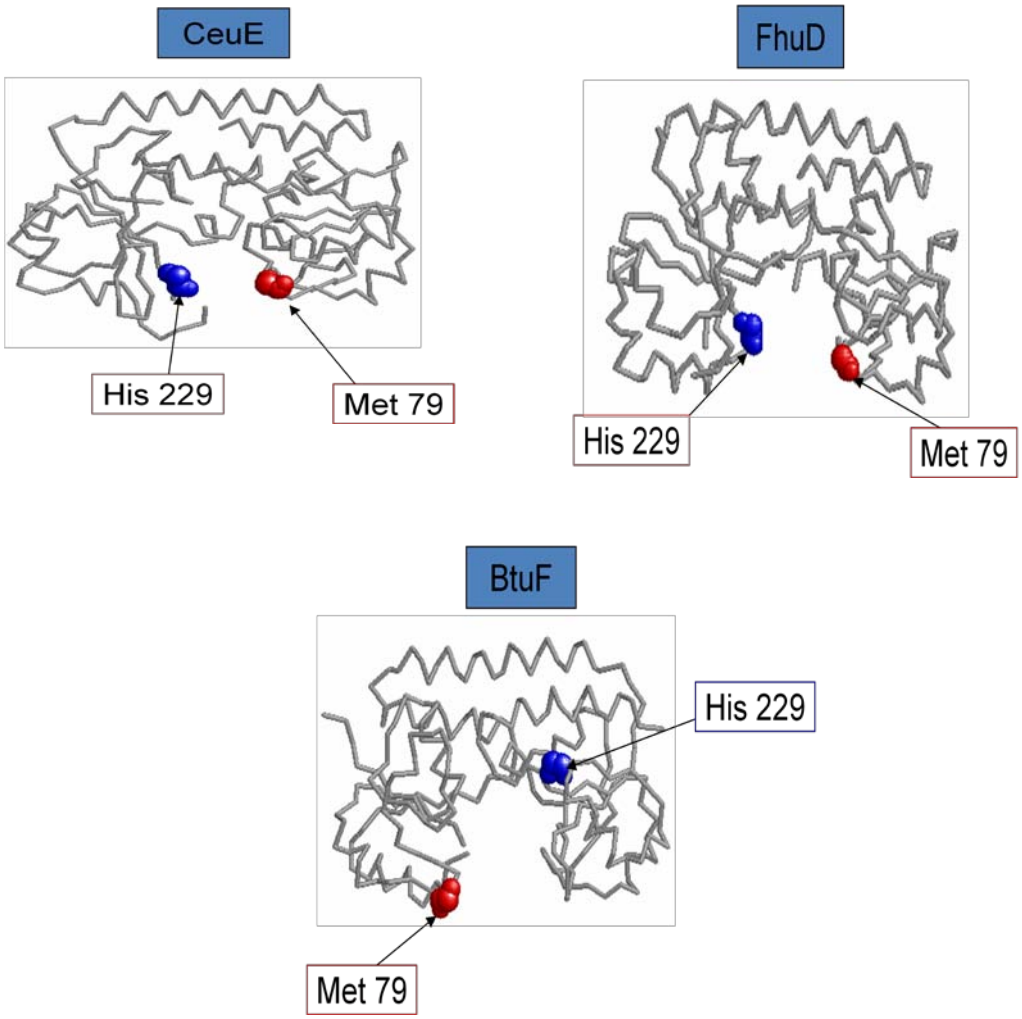

Figure 4. SiaA homology modeling. The SiaA sequence was threaded into homologous sequences with known crystal structures using the program LOOPP. Three models of SiaA were obtained: BtuF (1N2Z_A) (Borths et al., 2002), CeuE (2CHU_A) (Muller et al., 2006), and FhuD (1K7S_N) (Clarke et al., 2002). The structures were visualized using Rasmol.

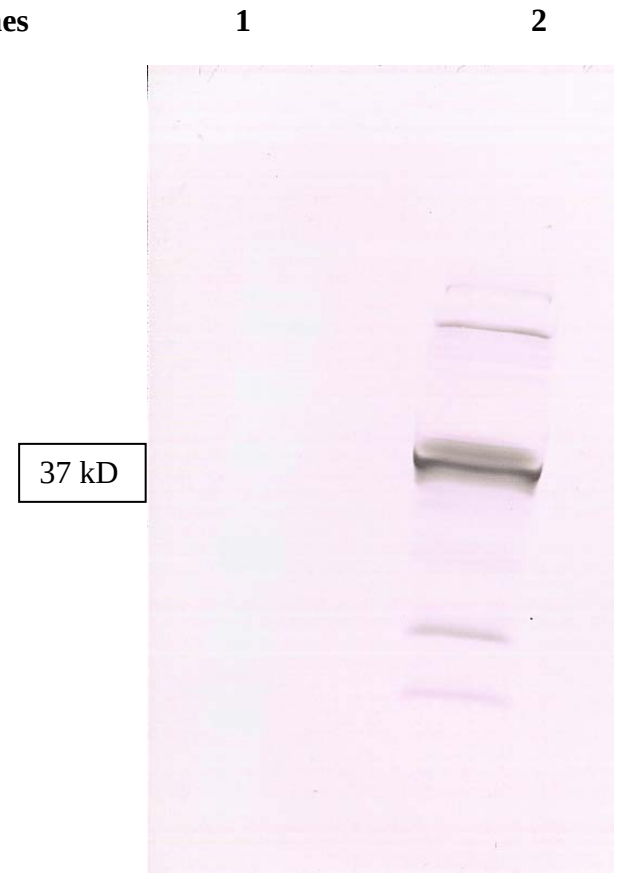

Figure 5. Western Blot of SiaA. Lane 1: Protein ladder. Lane 2: H229A grown in *E. coli*. The antibodies antiSiaA and antirabbit were used. The heavy band at 37 kD is H229A SiaA.

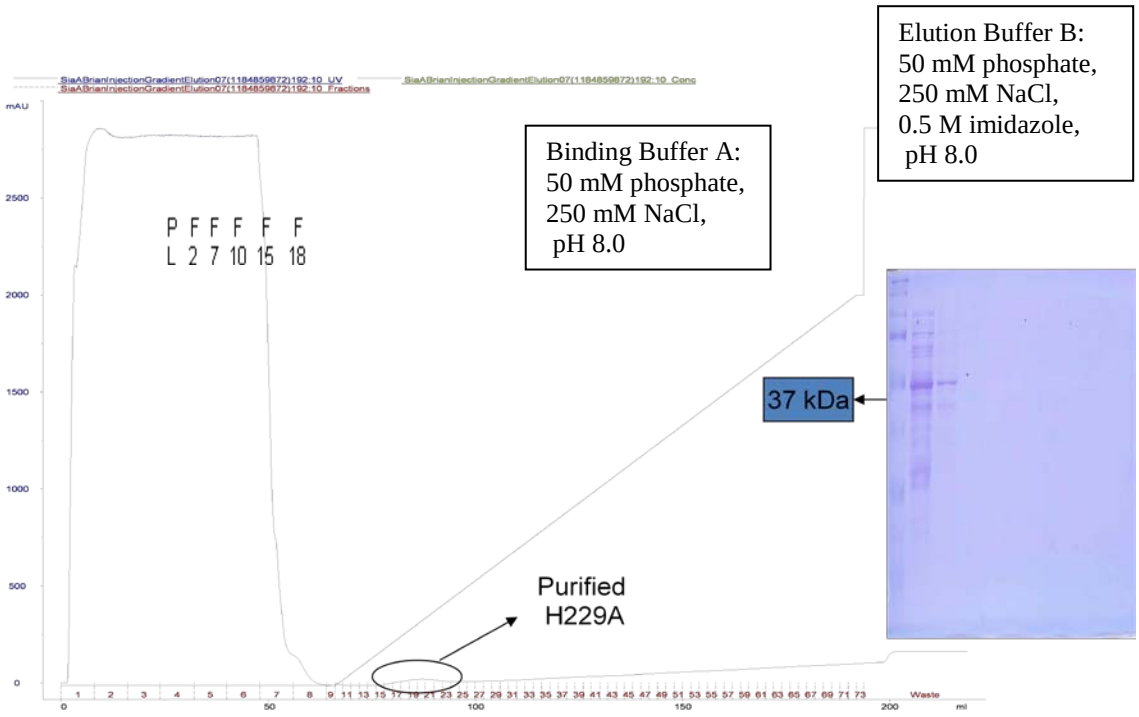

Figure 6. FPLC purification of the mutant of SiaA H229A. A nickel column affinity was used. Buffers A and B were the binding and elution buffers, respectively; the trace was visualized at 280 nm. Fractions 17-21 were collected and centrifuged. A light band was seen for the combined fractions on SDS PAGE.

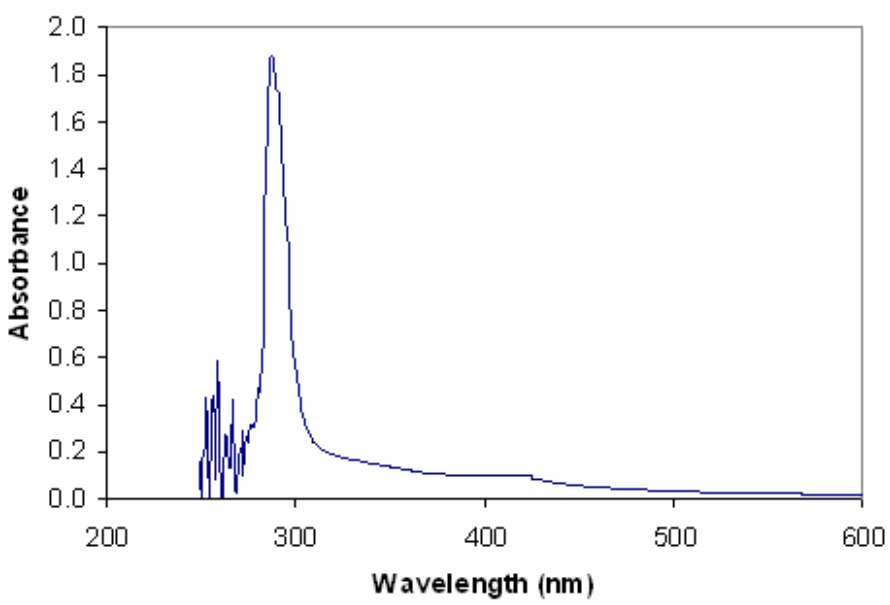

Figure 7. UV-visible spectrum of the H229A mutant after purification in 10 mM Tris-HCl buffer. The small size of the band at 420 nm with respect to the protein band at 288 nm indicates that heme is lost easily from this mutant.

CHAPTER 2. THE NEAT DOMAIN

2.1 *S. pyogenes* NEAT domains.

Another protein related to the ABC transporters discussed in Chapter 1.2 is Shr with a molecular weight of 139 kD (Aranda et al., 2007). UV-visible spectroscopy shows that Shr can bind heme as demonstrated by a peak at 410 nm. Shr contains two NEAT domains (Aranda et al., 2007; Zhu et al., 2008a; Zhu et al., 2008a). Shr binds and transfers beme to apo Shp. However, this heme binding protein does not transfers heme efficiently to apo SiaA.

The goal of this work was to prepare the second of these NEAT domains, designated herein as NEAT2 for characterization. The text below summarizes the other known heme binding NEAT domains.

2.2 Discovery of the NEAT domain.

The "NEAr Transporter" (NEAT) domain, a conserved region of approximately 125 amino acids, was discovered by sequencing genomes of pathogenic bacteria related to iron transport (Andrade et al., 2002). The composition of the NEAT domain is mostly β strands. Approximately, 80% of the residues are conserved in the β strands. NEAT domains have an amino-terminal signal sequence and a carboxy-terminal transmembrane region.

A single gene can have one or more NEAT domains. For example, *S. aureus* has two NEAT domains in *S_aur2*, one in *S_aur4*, and one in *S_aur3*. The total number of NEAT domains varies in different species. For example, *S. pyogenes* has two NEAT domains, whereas *B. halodurans* has six NEAT domains. The loops between the beta strands vary in the number of residues in different NEAT domains. For instance, between β 4 and β 5 the loop goes from 1 residue in *L mon2* to 19 residues in *L inn1* (Andrade et al., 2002).

2.3 *Staphylococcus aureus* NEAT domains

Staphylococcus aureus is a Gram positive pathogenic bacterium that contains a system of iron-regulated surface determinant (Isd) proteins which are involved in the acquisition of heme and iron (Grigg et al., 2007b). The system of Isd proteins is similar to the ABC transport system of *S. pyogenes*.

Staphylococcal strains that do not contain proper Isd systems were found to have fewer infections in mice than wild type strains (Pilpa et al., 2009). This lead to the assumption that Isd systems form part of the virulence system since the infections in mice were fewer when the Isd systems were not working correctly.

The Isd heme pathway acquisition involves nine proteins (Pilpa et al., 2009). Four of them are receptors (IsdA, IsdB, IsdC, and IsdH) which bind heme by NEAT domains. Not all the NEAT domains in *S. aureus* bind heme (Cavallaro et al., 2008). For example, *S. aureus* str MRSA2525 has three proteins that contain one or more NEAT domains, but only one of these proteins can bind heme (Cavallaro et al., 2008).

IsdA, IsdB, and IsdH are attached by Sortease A and IsdC by Sortease C to the cell wall (Clarke & Foster, 2008). IsdB and IsdH bind methemoglobin (MetHb) and IsdA binds heme and other ligands (Pilpa et al., 2009). After heme is bound to these proteins, heme is transferred to IsdC (Muryoi et al., 2008). IsdC transports heme to the IsdDEF system which delivers heme into the cytoplasm (Pilpa et al., 2009). The last step is thought to involve IsdG or IsdI, which cleaves the tetrapyrrole ring, releasing iron (Pilpa et al., 2009).

2.3.1 IsdA NEAT domain

IsdA contains one NEAT domain that binds heme. UV-visible spectroscopy shows that IsdA NEAT domains can bind heme as demonstrated by a peak at 407 nm (Grigg et al., 2007b). The axial ligand for IsdA is Tyr166. The crystal structure of apo and holo IsdA NEAT domain

structures do not show major differences (Grigg et al., 2007b). Mass spectrometry indicates that IsdA apo NEAT has a series of peaks centered around a charge distribution of +8. IsdA holo NEAT has a charge distribution peak of + 8. The presence of hemin does not change the charge distribution; this led to the assumption that there is not major conformational change in the protein when it binds heme (Grigg et al., 2007b).

2.3.2 IsdB NEAT domain

IsdB is a surface protein anchored to the cell wall (Pishchany et al., 2009). IsdB contains two NEAT domains; $IsdB^{N1}$ with 130 and $IsdB^{N2}$ with 126 amino acids (Pilpa et al., 2009). $IsdB^{N1}$ has more similarities with $IsdH^{N1}$ and $IsdH^{N2}$, whereas $IsdB^{N2}$ has more similarities with $IsdH^{N3}$. Both IsdB NEAT domains act as receptors for heme. IsdB binds heme from hemoglobin and not free heme (Torres et al., 2006). IsdB can obtain heme from hemoglobin and transport it to IsdA (Muryoi et al., 2008; Zhu et al., 2008a; Pishchany et al., 2009).

2.3.3 IsdC NEAT domain

IsdC is a surface protein anchored to the cell wall. IsdC contains one NEAT domain that binds heme. IsdC can obtain heme from both hemoglobin and from other sources (Pilpa et al., 2009). The crystal structure of the heme-bound NEAT domain of IsdC (Figure 11) shows eight β-sheets, one α-helix, and nine to ten loops. IsdC has a five coordinate heme center with Tyr132 as the axial ligand (Villareal et al., 2008). Pluym et al. have investigated the conformation of IsdC using mass spectroscopy (Pluym et al., 2008). The apo form of the NEAT domain in IsdC has two charge distribution peaks of +8 and +9. The holo form of the NEAT domain also has charge distribution peaks of +8 and +9 (Pluym et al., 2008). The observation that the charge distribution peaks remains the same in the apo and holo forms leads to the assumption that there is no major conformational change in the protein when it binds heme (Pluym et al., 2008).

Electron spray ionization mass spectrometry (ESI-MS) has also been used to probe heme transfer. Experiments show that heme is transferred to the NEAT domain of apo IsdC from the holo NEAT domains of IsdA, IsdB, and $IsdH^{N3}$ (Muryoi et al., 2008). For example, when the NEAT domain of apo IsdC was mixed with NEAT domain of holo IsdA, the spectrum showed peaks for apo IsdC (14442 amu), apo IsdA (14626 amu), and holo IsdC (15059 amu). The absence of the holo IsdA indicates heme transfer from holo IsdA to apo IsdC.

2.3.4 IsdH NEAT domain

IsdH contains three NEAT domains. $IsdH^{N1}$, $IsdH^{N2}$, and $IsdH^{N3}$ are composed of 144, 143, 126 amino acids, respectively (Muryoi et al., 2008). $IsdH^{N1}$, $IsdH^{N2}$ and $IsdB^{N1}$ have conserved amino acids and share a 46-65% identity (Pilpa et al., 2009). $IsdH^{N1}$ and $IsdH^{N2}$ are known to bind methemoglobin (MetHb) and haptoglobin (Hp); the third domain $IsdH^{N3}$ was found to bind heme from MetHb (Pilpa et al., 2009). As isolated from culture, only $IsdH^{N3}$ showed a Soret band (412 nm) (Watanabe et al., 2008).

The crystal structure of $IsdH^{N3}$ shows three α-helices and eight β-strands (Watanabe et al., 2008). This protein has a five coordinate heme center with Tyr642 as the axial ligand of the iron. Mutation of Tyr642 to alanine showed a shift in the Soret band. However, heme still appeared to bind.

2.4 δ-Aminolevulinic Acid

δ-Aminolevulinic acid (ALA) is a heme precursor which is often used in expression of proteins to promote the production of holo protein (Austin et al., 2004). The synthesis of ALA is the first committed step in the synthesis of heme (Cavallaro et al., 2008; Heinemann et al., 2008). Succinyl CoA and glycine condense to form ALA, releasing CoA and CO_2. ALA is added to the culture before the inducer. Several proteins have shown an increase in holo protein production

when ALA is used during expression. Optimization experiments are carried out for each protein in order to determine the amount of ALA that must be added during the expression. Often, iron is added along with the ALA to ensure that there is sufficient free iron to synthesize heme (Austin et al., 2004).

An example of a successful use of ALA is in the production of indoleamine 2,3-dioxygenase (IDO), an enzyme involved in tryptophan metabolism (Austin et al., 2004). IDO expression with addition of hemin yielded 1.4 mg of protein per 1 L broth. Austin and co-workers also expressed the protein using various concentrations of ALA and ALA along with ammonium iron (III) citrate. The addition of iron did not increase the yield of protein. ALA was added to give final concentrations ranging from 0.1 to 1 mM. The ALA concentration yielding the greatest protein activity was 1 mM ALA (~20 µmol/h/mg of protein). However, they found that 1 mM ALA was the upper limit that this bacterium could tolerate and therefore used 0.5 mM ALA for expression, yielding ~ 14 µmol/h/mg (Austin et al., 2004). The optimized expression gave 3.5 mg IDO per 1 L broth. A second example is hydroperoxide lyase P450 cytochrome (Delcarte et al., 2003). The addition of iron did not increase the amount of protein. However, the addition of 2.5 mM ALA doubled the amount of protein (Delcarte et al., 2003). In general, ALA produces higher expression yields of cytochromes P450.

2.5 Experimental

Luria-Bertani Agar (LB, 500 mL) was made by mixing 5 g sodium chloride (NaCl) (Aldrich Chemicals, Milwaukee, WI), 5 g of tryptone (Becton Dickinson, Sparks, MD), 2.5 g of Bacto™ yeast extract (Becton Dickinson), 10 g agar (Becton Dickinson), and 18 MΩ water (Barnstead NANOpure Diamond purifier) (VWR, Batavia, IL) to a final volume of 500 mL. The pH was adjusted to 7.04 with NaOH. The solution was autoclaved (Amsco remanufactured 3021 gravity

sterilizer) on a liquid cycle for 15 min, cooled to room temperature. A total of 400 µl of ampicillin (AMP) (100 mg/mL stock solution) [(made by diluting 1 g of AMP sodium salt (Fisher Scientific, Fair Lawn NJ) to 10 mL sterile water] was added to the broth. The solution was poured into 11 Petri dishes.

NEAT2 plate inoculation. Using aseptic techniques, Strep-tag Shr-ddNEAT2 [a gift from Dr. Eichenbaum (Georgia State University)] was inoculated into two LB agar plates. These plates were incubated overnight at -20 ºC.

LB medium preparation. A batch of LB medium was made by adding 15 g tryptone, 7.5 g Bacto^{TM} yeast extract, 15 g NaCl, and 1500 mL water to a 2.8 L Erlenmeyer flask. The pH was adjusted to 7.01 by addition of aqueous NaOH. The solution was autoclaved using the liquid cycle for 15 min and cooled to room temperature. A total of 1.5 mL AMP stock solution was added to the LB medium. LB medium (30 mL) was added to a 125 mL Erlenmeyer flask.

LB medium inoculation and growth of NEAT2. Under sterile conditions, Strep-tag Shr-ddNEAT2 was added with an inoculating loop to the LB medium (30 mL) solution in a 125 mL Erlenmeyer flask. The solution was shaken overnight (~16 h) at 37 °C and 225 rpm. The remaining LB solution (~1470 mL at room temperature) was mixed with the inoculated solution at which the OD_{600} was about 0.07. The solution was shaken for 7.5 h at 30 °C and 225 rpm to a final OD_{600} of 0.6. A total of 150 µL of anhydrotetracycline (AHT) (made by adding 2 mg/mL to a final concentration of 200 ng/mL) was added to the LB broth. The LB broth was shaken overnight (~16 h) at 27 ºC and 225 rpm. The culture broth was evenly distributed into 1 L sterile plastic centrifuge bottles and centrifuged at 8000 x g for 5 min at 4 °C. The supernatant was discarded and the cell pellet was stored in the -80 °C freezer.

Addition of ALA and iron sulfate heptahydrate ($FeSO_4 \cdot 7\ H_2O$) to the LB medium. Under sterile conditions, Strep-tag Shr-ddNEAT2 was added with an inoculating loop to the LB medium (30 mL) solution in a 125 mL Erlenmeyer flask. The solution was shaken overnight (~16 h) at 37 °C and 225 rpm. The remaining LB solution (~1470 mL at room temperature) was mixed with the inoculated solution at which the OD_{600} was about 0.07. The solution was shaken until an OD_{600} of 0.3. ALA (Acros Organics, New Jersey USA) was added to a final concentration of 103 µM and $FeSO_4 \cdot 7\ H_2O$ (Aldrich Chemical Company, Milwaukee, WI) was added to a final concentration of 40 µM to the broth at a 0.4 OD_{600}. The solution was shaken at 30 °C and 225 rpm to a final OD_{600} of 0.6. A total of 150 µL of 200 ng/mL AHT was added to the LB broth. The LB broth was shaken overnight (~16 h) at 27 ºC and 225 rpm. The culture broth was evenly distributed into 1 L sterile plastic centrifuge bottles and centrifuged at 8000 x g for 5 min at 4 °C. The supernatant was discarded and the cell pellet was stored in the -80 °C freezer.

Modified Lowry Protein Assay. A Modified Lowry Protein Assay kit (Pierce, Rockford, IL) was used for this experiment. Diluted albumin (BSA) standards were prepared to construct a standard curve. The specific volumes for the solutions used for the standards were listed in a table in the manual of the kit. A total of 0.2 L of purified NEAT2 was added to an Eppendorf tube. At 15 s intervals between each sample including the standards, 1 mL of Modified Lowry Reagent (provided by the kit) was added. The samples were incubated for 10 min at room temperature. A total of 100 µL of 1X Folin-Ciocalteu Reagent [made by diluting 2X (2N) reagent (provided by the kit) with water in a 1:1 ratio] was added to each sample including the standards. The samples were incubated for 30 min at room temperature. The absorbance of all the samples was measured via UV-visible spectroscopy at 750 nm. The blank standard was used

to correct the absorbance of the rest of the samples. The BSA standards were used to construct a standard curve by plotting absorbance vs. concentration (µg/mL). The concentration of the samples at 750 nm was calculated from the standard curve. The total amount of holo NEAT2 was calculated multiplying the concentration of the sample and the total amount of the sample (200 µL). The amount obtained from this assay was compared to the sample obtained in UV-visible spectroscopy for some samples.

FPLC (Fast Protein Liquid Chromatography). Buffer A 10X (150 mL) was prepared by adding 13.1 g NaCl, 18.1 g Tris-Cl and 150 mL autoclaved water in an Erlenmeyer flask. The pH was adjusted to 8.09 with HCl. The solution was filtered using a how Nalgene disposable bottle top filter 150 mL 0.45 µm pore size. Buffer A (500 mL) was prepared with 50 mL Buffer A 10X and 450 mL water. Buffer B (100 mL) was prepared by adding 0.06 g of desthiobiotin (Sigma-Aldrich, St. Louis, MO) and 100 mL of Buffer A. Buffer R (200 mL) was prepared by adding 0.04 g 2-(4-Hydroxyphenylazo) benzoic acid (HABA) (Sigma-Aldrich) and 200 mL of Buffer A.

The superloop was washed with water and pump A and B were washed with buffer A and B, respectively. The Strep Tactin Superflow high capacity column (Strep-tag) (IBA, St. Louis, MO) with a 5 mL bed volume was washed with 50 mL buffer A. The column was regenerated with buffer R. The protein in solution was inserted to the system with a syringe. A step gradient method was used with 5 column volumes.

UV-visible spectroscopy. A Cary 50 Bio UV-visible spectrophotometer was used for all the absorbance determinations. To each 100 µL of protein, 300 µL of 20 mM Tris-Cl 10% glycerol buffer (recipe) were added in a 6Q cuvette. The base line was done with the blank sample that contained the buffer 20 mM Tris-Cl 10% glycerol. The range used for the spectrum was 800 –

250 nm. To calculate the amount of holo NEAT2 in the sample the absorbance at the Soret band was measured and the molar absorptivity used was 1.0×10^5 $M^{-1}cm^{-1}$.

2.6 Results and Discussion

2.6.1 Optimization of NEAT2

The goal of this work was to determine conditions that would yield substantial amounts of holoprotein for spectroscopic studies. Holoprotein would also be needed to pursue x-ray studies, as it is significantly easier to solve the structure when the crystal has only holoprotein, rather than a mixture of holo- and apo-protein.

As outlined in the Materials and Methods section, several variables were changed in order to determine which change will yield greater amounts of protein, as well as the highest amount of holoprotein. Ten different experiments were run, and the amount of holoprotein (in mg) calculated for each one.

Experiment I involved the standard conditions in use in the laboratory when this work began. Figure 12 shows the cultures both before and after French press. It can be seen that the majority of the protein is the desired NEAT2 (21 kD) (lane 2) and that very little is released upon French pressing (lane 3). This presumably indicates that most of the protein is in inclusion bodies. The purity of the protein is indicated both by the SDS-PAGE (Figure 12) as well as the FPLC purification of the experiment (Figure 13). However, an SDS-PAGE run after FPLC purification indicates that the protein shows an additional band that is of slightly lower molecular weight (lane 2 of Figure 14). This may be due to proteolytic cleavage of the protein.

The spectrum of the protein from Experiment I (Figure 15) indicates that it is approximately 52% holo protein (calculated from the 404 to 280 ratio of 1.30 and assuming a fully holo ratio of 2.5). The shoulder at 422 nm is very probably due to the reduced form of the

protein, which has been shown to absorb 429 nm (Figure 16). To see what would happen with more available oxygen, growth was performed with half the amount of media (Experiment II). Using the same shaking flask, this results in more surface area, and hence the option for more oxygen to diffuse into the culture. Figure 12 compares the cultures from Experiment I and II both before and after French press. It can be seen that reducing the volume of culture (increasing the available oxygen) reduces the amount of NEAT2. The two experiments result in protein of comparable purity as seen the SDS-PAGE (Figure 12 and in comparing the FPLC traces (Figures 13 and 17). The spectrum of the protein (Figure 18) indicates that is it approximately 26% holo protein (calculated from the 404 to 280 ratio of 0.64).

The next experiment (Experiment III) involved growth at higher temperatures to see if this would result in more protein. Specifically, the pre-culture, growth and after-inducer temperatures were 34, 34, and 31 °C in comparison with the 30, 30 and 27 °C of Experiment I. The SDS-PAGE before and after French press (lanes 2 and 3, respectively, of Figure 19) shows that again, the protein is difficult to extract from the cells although there seems to be some more protein in the supernatant of Experiment III in comparison to Experiment I. The protein appears somewhat less pure in the SDS-PAGE (Figure 19) and also shows a leading small band in the FPLC (Figure 20). The amount of holo protein calculated from the UV/vis spectrum (Figure 21) was 0.39 g/L. The smaller amount of protein in comparison with Experiment I, and the indications that it may not have been as pure, show that increasing the temperature was not a successful route to high yields of holoprotein. Figure 14 shows the SDS-PAGE of NEAT2 from Experiment II after FPLC purification. It can be seen that there are two heavier bands in the gel, one at about 40 kD and the other at about 60 kD. This is also in line with the observation that the protein may not be as pure as that isolated in Experiment I. However, there is another possibility.

In a native gel, NEAT2 can be seen to form oligomers (Figure 22, data courtesy of Y. Zhuo). It is possible that these heavier bands on the SDS-PAGE represent oligomers of NEAT2. If they do, then the protein undergoes exceptionally tight self-association.

Experiment IV involved a high temperature for the pre-culture period (37 as opposed to 30 °C) and a slightly lower temperature after induction (25 as opposed to 27 °C). The SDS-PAGE (Figure 23, lane 2) shows a large amount of pure protein of the desired molecular weight. The FPLC (Figure 24) also indicates that the protein is pure. A MALDI mass spectrum was performed of this protein (Figure 25). The observed mass (21758.2) is within 0.2% of the predicted mass (21706.2), assuming cleavage between the Q and A in the sequence AQAAS. The cleavage is performed by cellular proteases, and the exactly cleavage site is not known *a priori*, but this mass spectrum is consistent with the desired protein. The UV/visible spectrum indicated significant amount of the ferrous protein, as seen in the band at 429 nm (Figure 26).

Experiment V involved a high temperature for the pre-culture period (37 as opposed to 30 °C) but lower temperatures for growth (25 as opposed to 30 °C) and a slightly lower temperature after induction (25 as opposed to 27 °C). The SDS-PAGE (Figure 23, lane 1) shows a significant band for the desired protein but also, as seen in Experiment III, a band at approximately 60 kD. Experiment V shows no band at approximately 40 kD, however. The FPLC (Figure 27) also indicates that the protein is pure. The UV/visible spectrum (Figure 28) indicated only a small amount of the ferrous protein, as seen in the shoulder at approximately 429 nm. The percent holoprotein, calculated from the 407 to 280 ratio of 2.28, was 91% Although the overall amount of protein was low (only 0.13 mg/L) this protocol gave the highest amount of holoprotein of Experiments I – V.

A second series of experiments (A – C) involved differences in the time after addition of the inducer AHT (in comparison with the 16 h of Experiment I). These experiments were run as in Experiment IV, but on a 1.0 L scale, and with an after inducer temperature of 27 °C. In Experiment A, only one hour was allowed between induction and centrifugation. Under these conditions, no NEAT2 was observed (data not shown).

In Experiment B, 16 h were allowed between induction and centrifugation. This protocol is the almost the same as Experiment IV, differing only in the amount of broth (1.0 vs. 1.5 L) and after inducer temperature (27 vs. 25 °C). The FPLC of this protein indicated that it is pure (Figure 29; there was no SDS PAGE for this experiment). The UV/visible spectrum (Figure 30) indicated significant amounts of the reduced form of the protein. Experiment B produced about 0.21 mg/L of holoprotein. It should be noted that Experiment B gave 0.21 mg/L of holo NEAT2 whereas the very similar Experiment IV gave 1.07 mg/L of holoprotein. The significant differences in protein isolated, even under very similar conditions, may indicate the difficulty of solubilizing the protein into the supernatant.

Experiment C was the same as Experiment B, but with 14 h allowed between induction and centrifugation. The FPLC of this protein indicated that it was pure (Figure 31; there was no SDS PAGE for this experiment). The UV/visible spectrum (Figure 32) showed almost entirely Fe(II) protein. Experiment C gave 0.79 mg/L of protein, much closer to Experiment IV than to Experiment B. This again may indicate the difficulty of solubilizing the protein into the supernatant.

A final set of experiments involved the addition of δ-aminolevulinic acid. As described above this is a precursor to heme; the addition of ALA, with or without iron, can produce significant additional amounts of holoprotein in certain systems. Experiment ALA involved the

growth of the bacteria in the presence of 103 µM ALA without added iron. The protocol followed Experiment B with the exception that it was run in 1.5 rather than in 1.0 L broth. Figure 33 lane 4 shows the NEAT2 after FPLC purification. It appears very pure. The FPLC (Figure 34) is consistent with this. The UV/visible spectra (Figures 35 and 36) show significant amounts of both oxidized and reduced protein. This experiment produced 0.87 mg/L holoprotein, which was less than both Experiment I and Experiment IV. Thus, for this system, the addition of ALA alone does not result in significant additional amounts of holoprotein.

The final experiment (Experiment ALA + iron) was the same as Experiment ALA, but with the addition of 40 µM ferrous sulfate. Figure 33 lane 7 shows that the NEAT2 after FPLC purification is pure. The FPLC (Figure 37) appears consistent with this. The UV/visible spectrum (Figure 38) is very similar to that of Experiment ALA. This experiment produced 0.67 mg/L holoprotein, similar to that of Experiment ALA. Even the addition of ALA and iron does not result in significant additional amounts of holoprotein.

2.6.2 Expression and Purification of NEAT2

All the SDS-PAGE for each experiment showed a band at 21 kD which is correspondent to the molecular weight of NEAT2. The SDS-PAGE shows a dark band at 21kDa before French press. After French press, a much lighter band appears at 21 kD. This same pattern happens for Exp I, II, and III. We believe that inclusion bodies are being formed during French press.
The single peak seen in the FPLC after addition of the eluting buffer shows the purification of NEAT2. SDS-PAGE was run for the peaks in order to determine the purity. The results indicate that the peak contains NEAT2 and does not show any other band at other weights. Therefore, it can be concluded that NEAT2 was purified.

To each batch that was grown, a UV-visible spectroscopy spectrum was taken to determine the amount of holo protein obtained. The spectra showed Soret bands ranging from 400-410 nm. This is the region where heme proteins appear. The UV-visible spectra also showed protein bands at 280 nm.

2.6.3 Calculation of Holo NEAT2 Protein Amount and Total Protein Using UV-visibleible Spectroscopy and the Lowry Assay

The amount of total protein in Experiments II and III was calculated using the Lowry Assay; the standard curve is shown in Figure 39. The amounts of NEAT2 were 0.74 and 0.47 mg/L, respectively. Using the program ProtParam tool (Gasteiger et al., 2005), the extinction coefficient for NEAT2 was calculated from the sequence to be 24,410 $M^{-1}cm^{-1}$ at 280 nm. The 280 nm bands of Experiments II and III had absorbances of 0.056 and 0.135, respectively. Given this extinction coefficient, and a molecular weight of 21706 kD, we calculate from the spectra that the amounts of proteins are 0.89 and 2.1 mg/L for Experiments II and III, respectively. Although these two ways of calculating the concentrations of total protein are of the same order of magnitude, there are still significant differences. We believe that the differences in the total protein calculated in these two ways arise from two issues. First, the actual extinction coefficient at 280 nm will be higher than that calculated from the sequence due to a contribution from the heme. Second, the spectra were probably too dilute for accurate calculations of this type (especially for Experiment II, which does not have a clearly resolved 280 band).

UV-visible spectrometry was used to calculate the amount of holo NEAT2 protein in each experiment. These calculations are inexact, because the extinction coefficient of pure NEAT2 is not yet known and because in each case the isolated protein is a mixture of Fe(II) and Fe(III). However, using a Soret to 280 nm ratio of 2.5, we can get an approximate idea of how much holoprotein is in each experiment. These values are given in Tables I – III.

2.6.4 Homology modeling.

To obtain a visual picture of NEAT2, the sequence of this protein from *S. pyogenes* was threaded into its closest homology for which an X-ray structure is known IsdA from *S. aureus*, using PyMol. Figure 40 shows the model. A tyrosine appears in an appropriate position to be the axial ligand. However, reduction potential studies (D. Block and K.R. Rodgers, North Dakota State University, unpublished) are not consistent with this conclusion. Additional spectroscopic and structural work will be necessary to understand this system. It is to be noted that some heme proteins have more than one axial ligand set depending on the circumstances.

2.6.5 Conclusions.

The focus of this work was to find conditions that optimized the production of holo NEAT2 for spectroscopic studies. We observed that significant amounts of protein were not found in the supernatant, and hence presumably are found in inclusion bodies. This difficultly of solubilizing the protein made accurate comparison of different protocols challenging. Increasing the amount of oxygen available to the bacteria seemed to inhibit protein production; the optimization experiment yielding the least amount of protein was Experiment II. The addition of ALA alone or ALA with iron can (but does not always) increase the amount of holoprotein in heme protein growth experiments. For NEAT2, neither ALA nor ALA plus iron increased the amount of holoprotein produced.

The time to induction may be more important. The original time for induction was approximately 16 h. When this amount of time was reduced to 14 h, the amount of holoNEAT2 increased significantly. The amount of holo protein increased from ~ 0.2 mg/L to ~ 0.8 mg/L. This seems a large change for a small difference in induction time, but indicates that induction time may be a significant variable in holoprotein production.

Probably the most significant variable is temperature. The optimization experiment that yielded the greatest amount of protein was Experiment IV, in which the temperature after the induction with AHT was decreased. Changing the temperature after induction to 25 °C produced a higher amount of holoNEAT2 than at 31 °C or 20 °C. These results show that temperature is one of the most important factors when it comes to the production of holoNEAT2.

Table 1. The yield of NEAT2 as a function of expression variables. Each experiment followed the general procedure outlined under the LB medium preparation, LB medium inoculation, and growth of NEAT2 as discussed in the Materials and Methods section.

Variables	**Experiment I**	**Experiment II**	**Experiment III**	**Experiment IV**	**Experiment V**
Tryptone (g)	7.5	3.8	15	15	15
Yeast extract (g)	3.8	1.9	7.5	7.5	7.5
NaCl (g)	7.5	3.8	15	15	15
Water (L)	0.75	0.38	1.5	1.5	1.5
Lysis buffer (mL)	20	10	40	40	40
Protease inhibitor tablets	2	1	4	4	4
Pre-culture temperature (ºC)	30	30	34	37	37
Growth temperature (ºC)	30	30	34	30	25
After inducer temperature (ºC)	27	27	31	25	20
Amount of holoNEAT2 (mg) using UV-visible spectroscopy	1.5	0.06	0.58	1.6	0.2
Amount of total protein using Lowry Assay (mg)	Exp not performed	0.28	0.71	Exp not performed	Exp not performed
Percent holoNEAT2	52	26	49	25	91
Amount of holoNEAT2 (mg/L)	2.0	0.16	0.39	1.07	0.13

Table 2. The yields of NEAT2 as a function of time after the addition of inducer. Each experiment was done in 1 L broth, with temperatures of 37 (pre-culture), 30 (growth), 27 (after inducer) ºC.

Variables	Experiment A	Experiment B	Experiment C
Time after addition of AHT (h)	1	16	14
Amount of holoNEAT2 (mg)	No protein observed	0.210	0.789
Percent holoNEAT2	-	28	35
Amount of holoNEAT2 (mg/L)	-	.210	0.789

Table 3. The yields of NEAT2 with ALA and iron. Each experiment was done in 1.5 L broth, with temperatures 37 (pre-culture), 30 (growth), 27 (after inducer) ºC, and 16 h induction time.

Variables	Experiment ALA	Experiment ALA + Iron
[ALA] µM	103	103
[$FeSO_4 \cdot 7H_2O$] µM	0	40
Amount of holoNEAT2 (mg)	1.3	1.0
Percent holoNEAT2	48	41
Amount of holoNEAT2 (mg/L)	0.87	0.67

MKKTAIAIAVALAGFATVAQAASWSHPQFEKSGGGGGLVPRGSRDRGPEFLNQKQ LRDGIYYLNASMLKTDLASESMSNKAINHRVTLVVKKGVSYLEVEFRGIKVGKML GYLGELNYFVDGYQRDLAGKPVGRTKKAEVVSYFTDVTGLPLADRYGKNYPKVL RMKLIEQAKKDGLVPLQVFVPIMDAISKGSGLQTVFMRLDWASLTTEKAKVV

OmpA leader – Strep tag – linker – thrombin cleavage site – N2

Figure 8. Shr-NEAT2 construct. This sequence is composed of the OmpA leader (outer membrane protein A, red), a Strep tag sequence used for purification (green), a linker (black), and a potential thrombin cleavage site (blue, thrombin cleavage would occur between arginine and glycine), and the sequence of NEAT2.

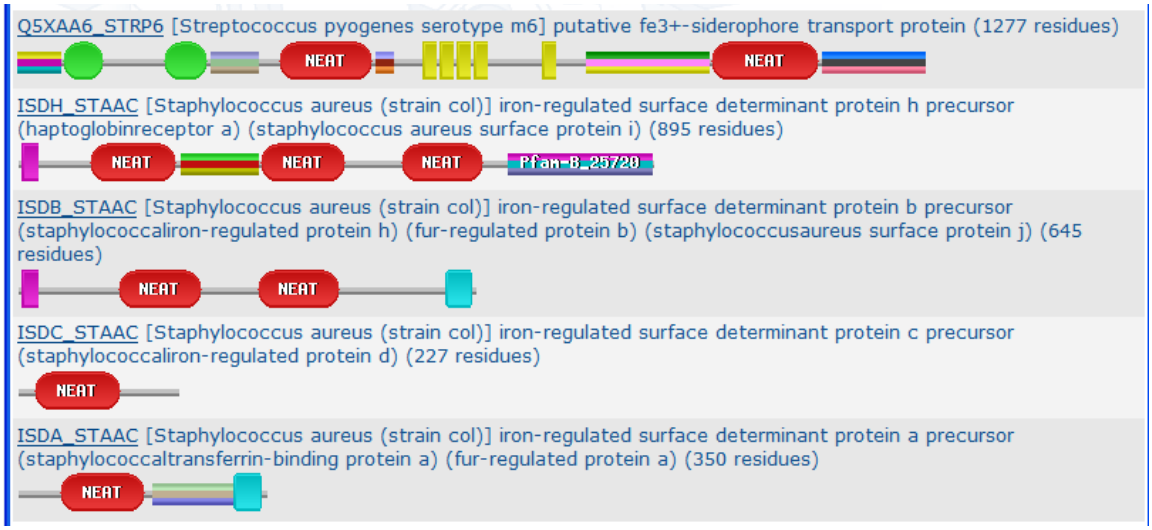

Figure 9. Representation of NEAT domains found in Shr (*S. pyogenes*, two NEAT domains), and the *S. aureus* proteins IsdH (three NEAT domains), IsdB (two NEAT domains), IsdC (one NEAT domain), and IsdA (one NEAT domain). These diagrams were generated using Pfam (Finn et al., 2008). The green circles are domains of unknown function (DUF); the yellow regions are leucine rich repeats; the light blue square in the C terminal region is a Gram positive anchor; and the purple square in the N terminal region represents the YSIRK-type signal peptide (Finn et al., 2008).

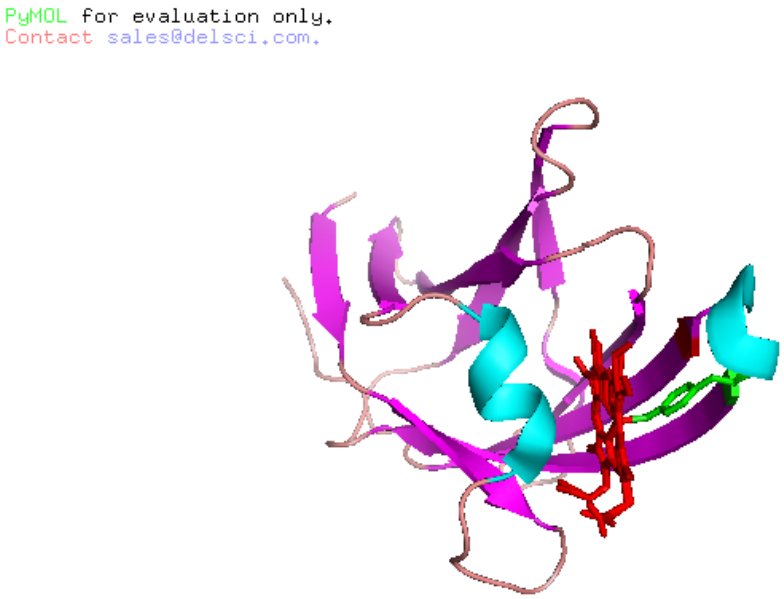

Figure 10. IsdA NEAT holo crystal structure (2ITF.pdb). Helices are shown in light blue, sheets are magenta, and loops are light pink. The axial ligand Tyr 166 is shown in green binding to heme which is red. Figure created in PyMOL from the data in (Grigg et al., 2007b).

Figure 11. IsdC NEAT holo crystal structure (2O6P.pdb), a closer look to the heme binding pocket. Helices are indicated with ribbons and colored light blue, beta sheets are indicated with arrows and colored magenta, and loops are light pink. The axial ligand, Tyr 132, is shown in green binding to heme which is red. Figure created by PyMOL from the data in (Sharp et al., 2007).

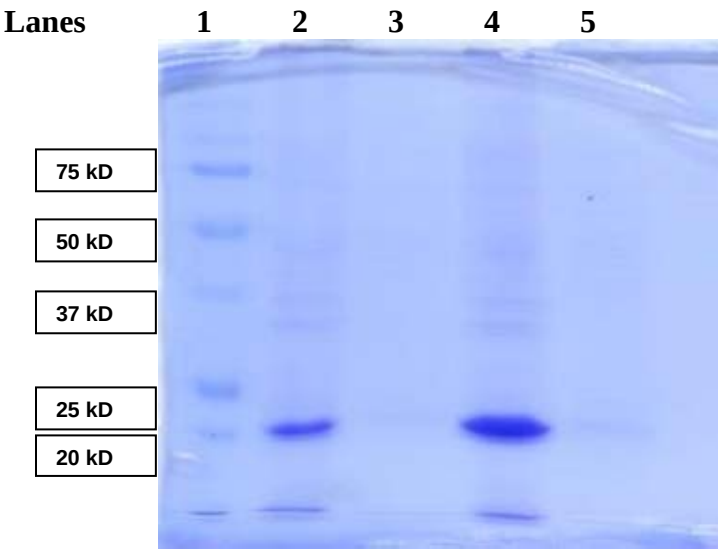

Figure 12. SDS-PAGE of NEAT2 grown in different amounts of broth. Lane 1: protein ladder. Lanes 2 and 3: NEAT2 grown in **Experiment II** [0.38 L culture (pre-culture, growth, and after-inducer temperatures of 30, 30, and 27 ºC, respectively)] before French press (lane 2) and after French press (lane 3). Lanes 4 and 5: NEAT2 grown in **Experiment I** [0.75 L culture (pre-culture, growth, and after-inducer temperatures of 30, 30, and 27 ºC, respectively)] before French press (lane 4) and after French press (lane 5).

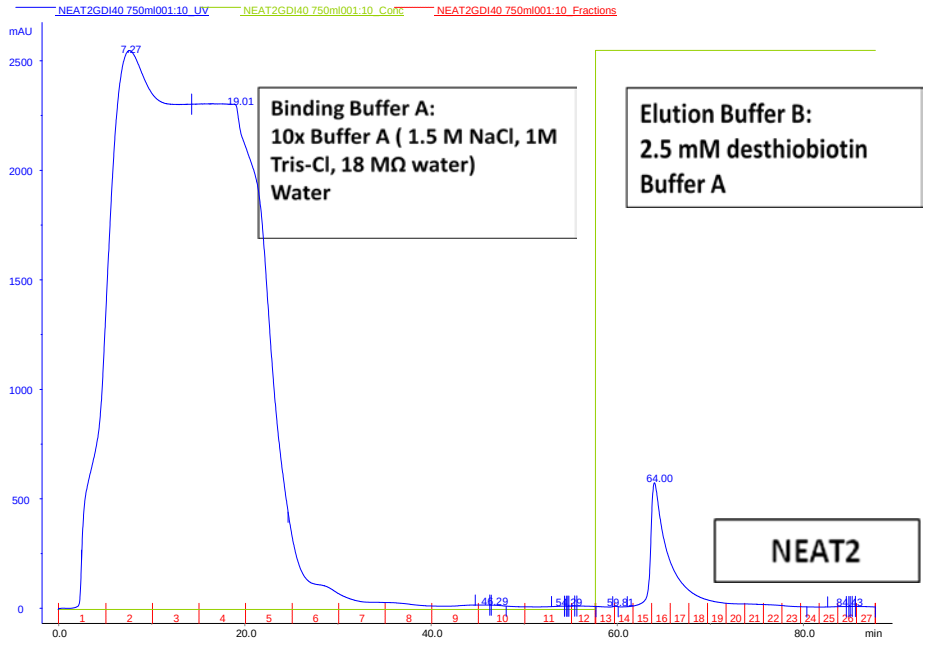

Figure 13. FPLC purification of NEAT2 grown in **Experiment I** by the stepwise method on a Strep Tactin Superflow high capacity column (IBA, St. Louis, MO, 5 mL). Buffers A and B were the binding and elution buffers, respectively. Fractions 15-19 were collected for centrifugation. Data taken at 280 nm.

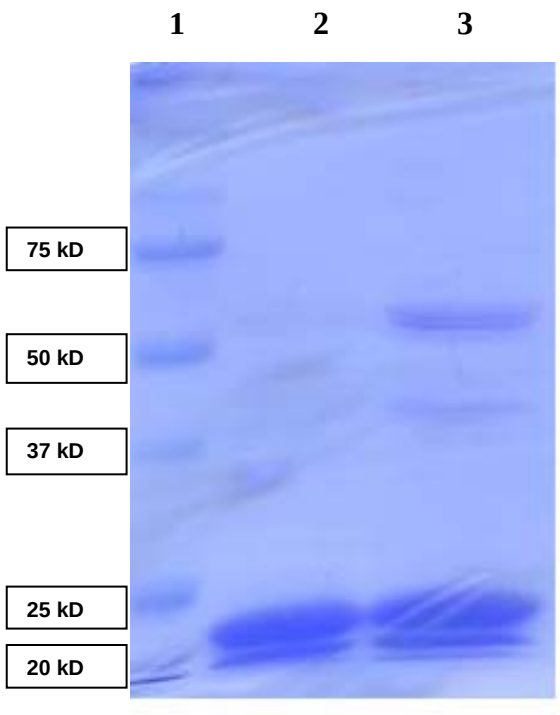

Figure 14. SDS-PAGE of **Experiment I** and **Experiment III**. Lane 1: protein ladder. Lane 2: NEAT2 grown in Experiment I after purification (0.75 L culture, pre-culture, growth, and after-inducer temperatures of 30, 30, and 27 ºC, respectively). Lane 3: NEAT2 grown in **Experiment III** after purification (1.5 L culture, (pre-culture, growth, and after-inducer temperatures of 34, 34, and 31 ºC, respectively).

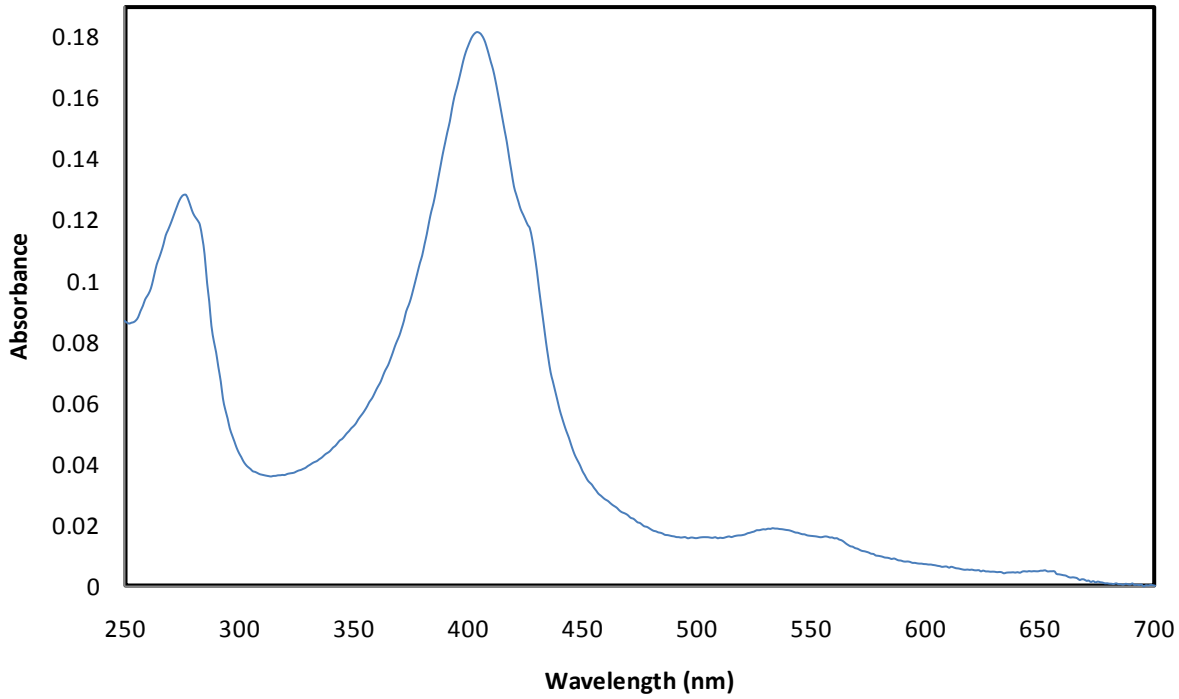
0.18
0.16
0.14
0.12
0.1
0.08
0.06
0.04
0.02
0
Absorbance
250
300
350
400
450
500
550
600
650
700
Wavelength (nm)

Figure 15. UV-visible spectroscopy of NEAT2 grown in **Experiment I** after purification (20 mM Tris, pH 8.0). The 404 to 280 ratio is 1.30. The shoulder at 422 nm is presumed to be the Fe(II) form of the protein. Maxima are also observed at 540, 560 and 652 nm.

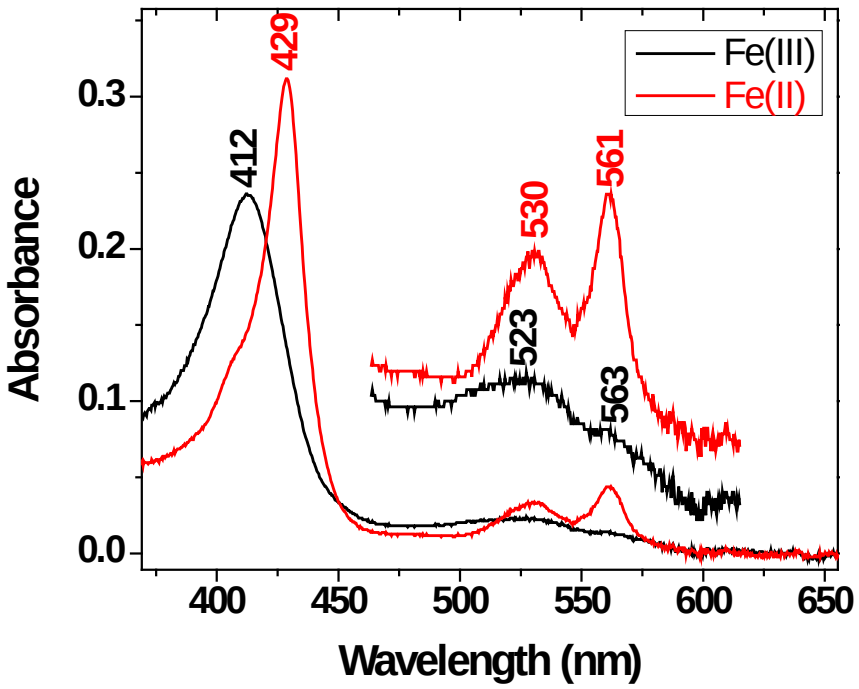

Figure 16. UV-visible spectra of oxidized (black) and reduced (red) NEAT2 in 50 mM Tris HCl, pH 8.0, 100 mM NaCl. Data taken by Darci Block in the laboratory of Dr. Kenton Rodgers.

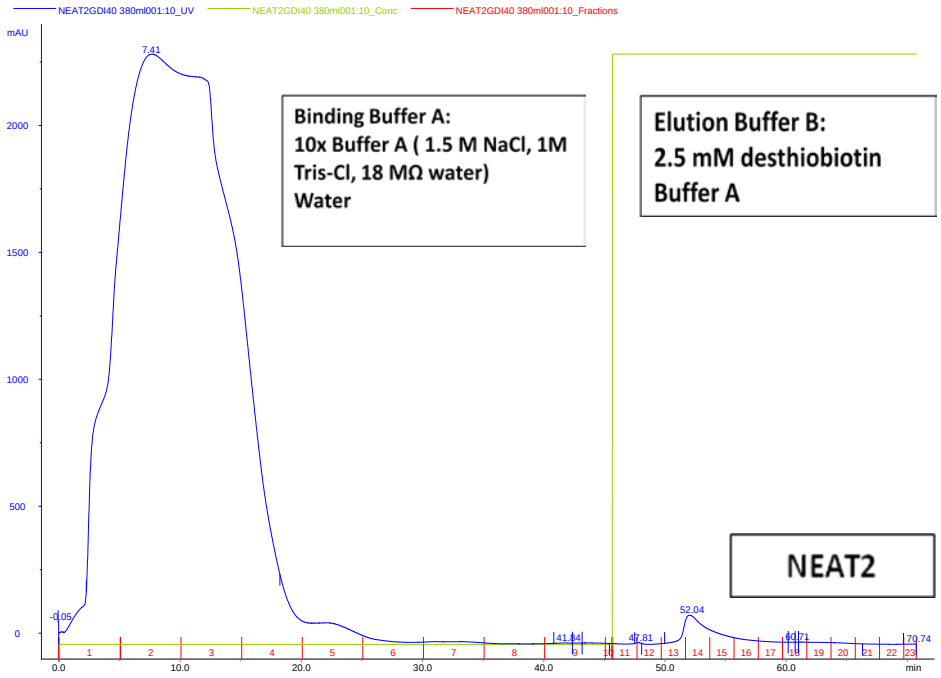

Figure 17. FPLC purification of NEAT2 grown in **Experiment II** by stepwise method on a Strep Tactin Superflow high capacity column (IBA, St. Loius, MO, 5 mL). Buffers A and B were the binding and elution buffers, respectively. Fractions 13-16 were collected for centrifugation. Data taken at 280 nm.

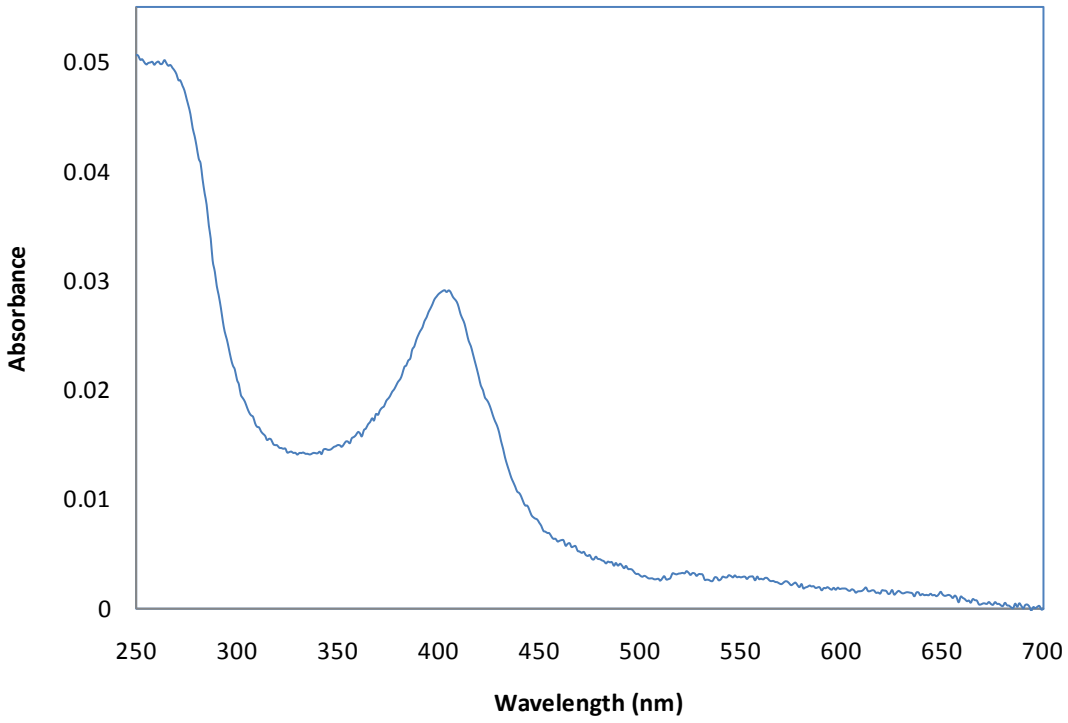

Figure 18. UV-visible spectrum of NEAT2 grown in **Experiment II** after purification (20 mM Tris, pH 8.0). The 404 to 280 ratio is 0.64.

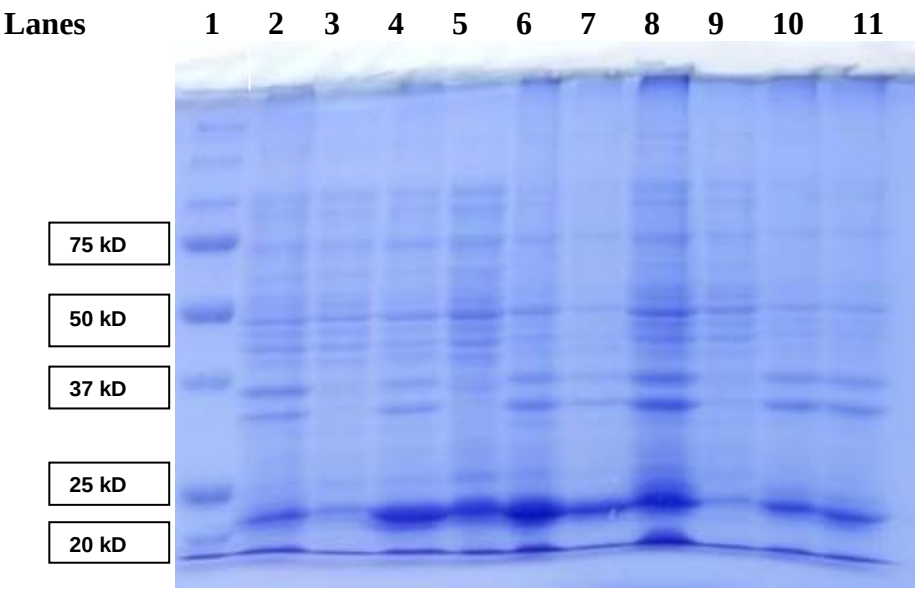

Figure 19. SDS-PAGE of NEAT2 grown with different temperatures, Experiments III and IV. Lane 1: protein ladder. Lanes 2 and 3: NEAT2 grown in **Experiment III** (pre-culture, growth, and after-inducer temperatures of 34, 34, and 31 ºC, respectively) before (lane 2) and after (lane 3) French Press. Lanes 4, 5, 6 and 7: NEAT2 grown in **Experiment IV** (pre-culture, growth, and after-inducer temperatures of 37, 30, and 25 ºC, respectively) before French Press (lane 4), after French Press (lane 5), Pellet 1 (lane 6), and Pellet 2 (lane 7). Lanes 8, 9, 10 and 11: NEAT2 grown in **Experiment V** (pre-culture, growth, and after-inducer temperatures of 37, 25, and 20 ºC, respectively) before French Press (lane 8), after French Press (lane 9), Pellet 1 (lane 11) and Pellet 2 (lane 12).

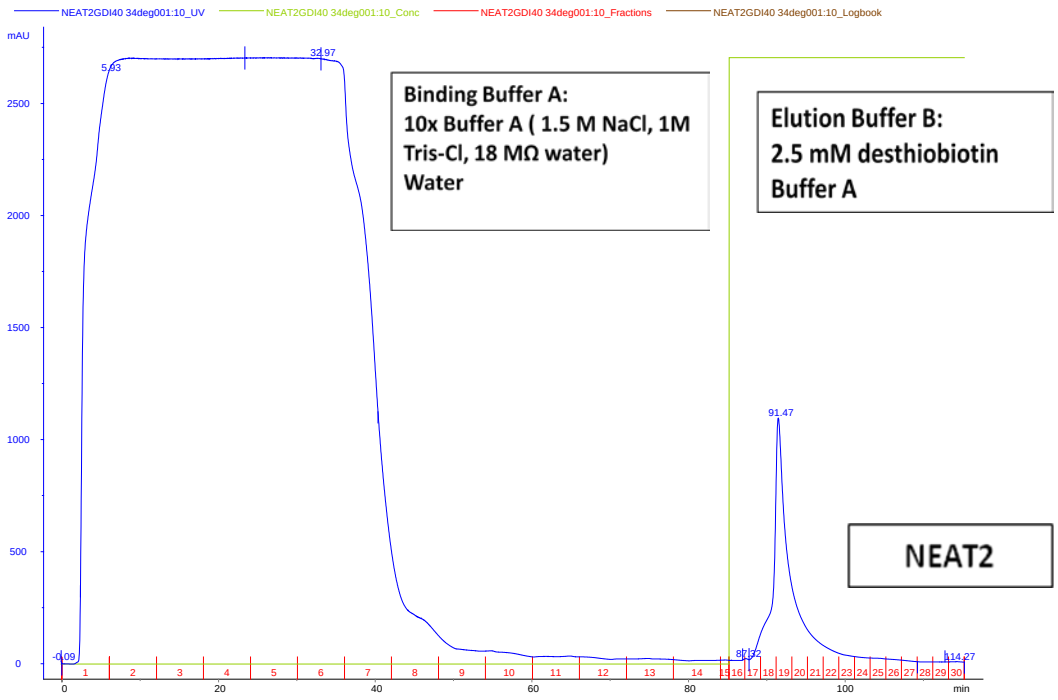

Figure 20. FPLC purification of NEAT2 grown in **Experiment III** by stepwise method on a Strep Tactin Superflow high capacity column (IBA, St. Loius, MO, 5 mL). Buffers A and B were the binding and elution buffers, respectively. Fractions 17-24 were collected for centrifugation. Data taken at 280 nm.

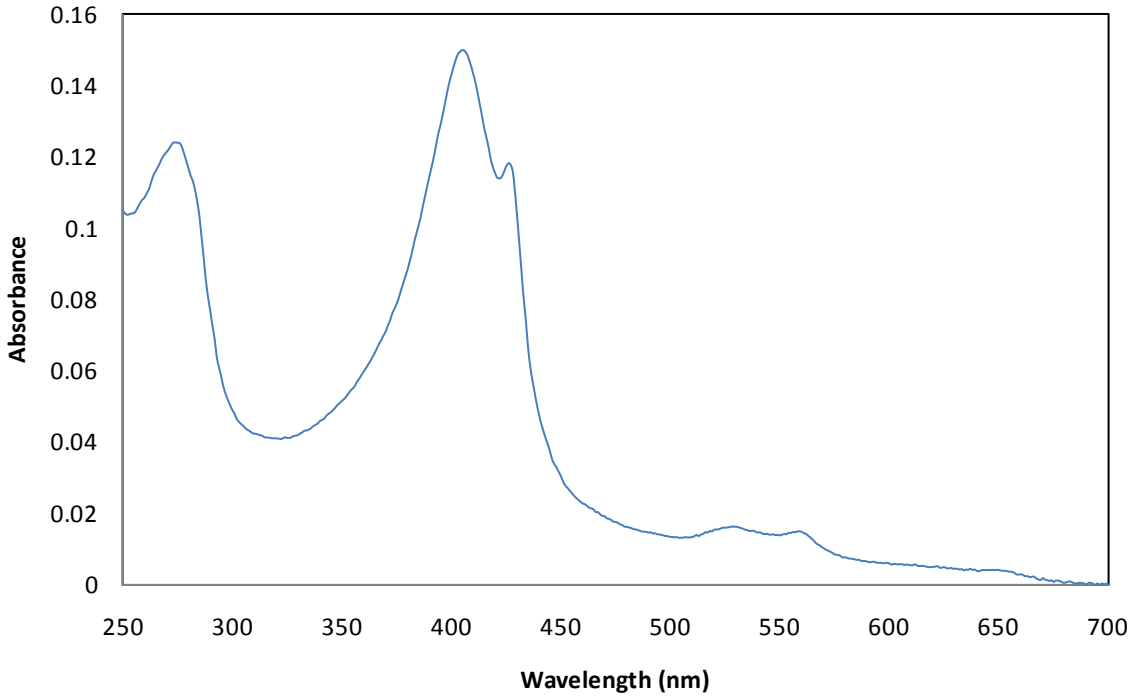

Figure 21. UV-visible spectrum of NEAT2 grown in **Experiment III** after purification in (20 mM Tris, pH 8.0). The 405 to 280 ratio is 1.23. The shoulder at 425 nm is presumed to be the Fe(II) form of the protein. Maxima are also observed at 527, 556 and 652 nm.

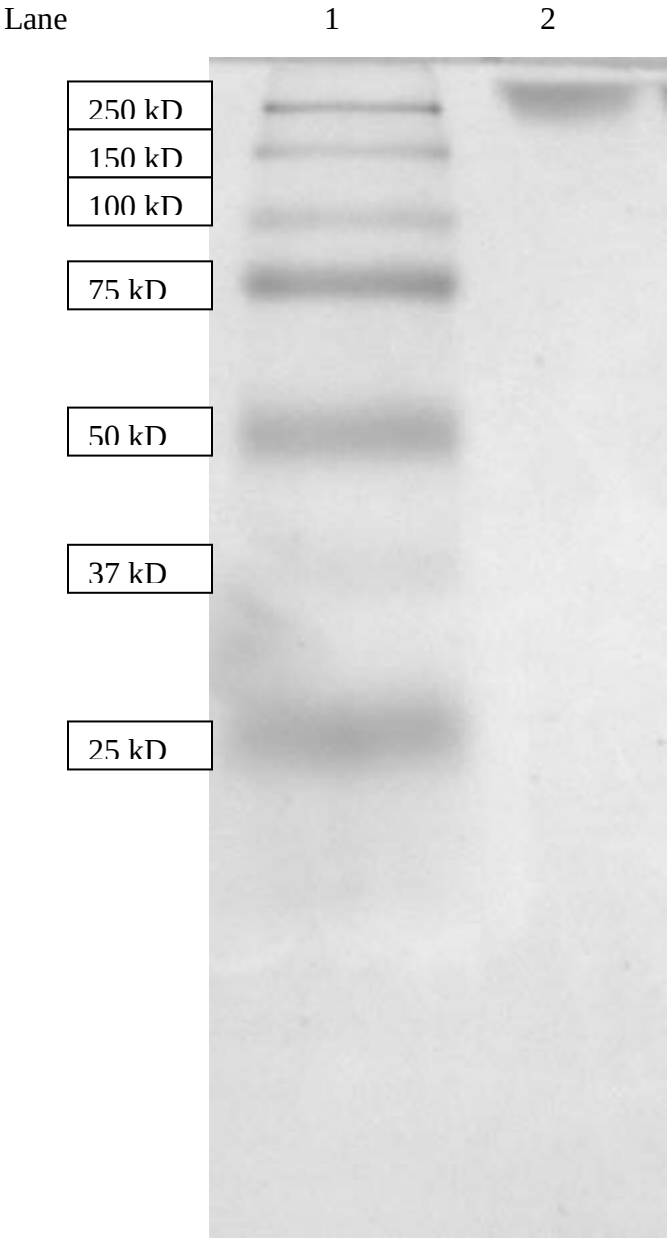

Figure 22. ZhuoNEAT2_ 6. ZYII40. Native PAGE. Lane 1: protein ladder. Lane 2: is NEAT2 (Delgado's sample Experiment C). Data taken by Y. Zhuo.

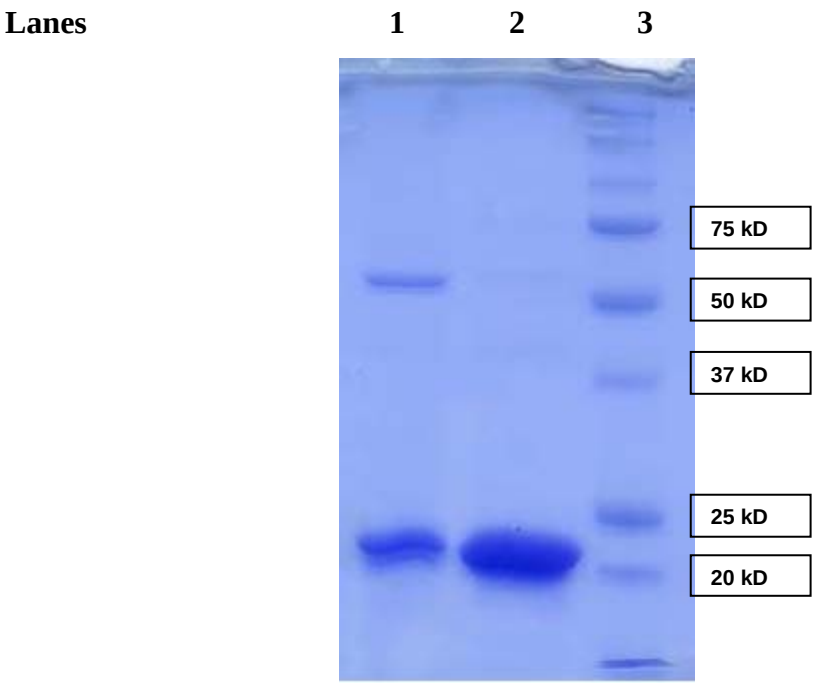

Figure 23. SDS-PAGE of NEAT2 grown with different temperatures, Experiments IV and V. Lane 1: NEAT2 grown in **Experiment V** (1.5 L culture, pre-culture, growth, and after-inducer temperatures of 37, 25, and 20 ºC, respectively). Lane 2: NEAT2 grown in **Experiment IV** (1.5 L culture, pre-culture, growth, and after-inducer temperatures of 37, 30, and 25 ºC, respectively). Lane 3: protein ladder.

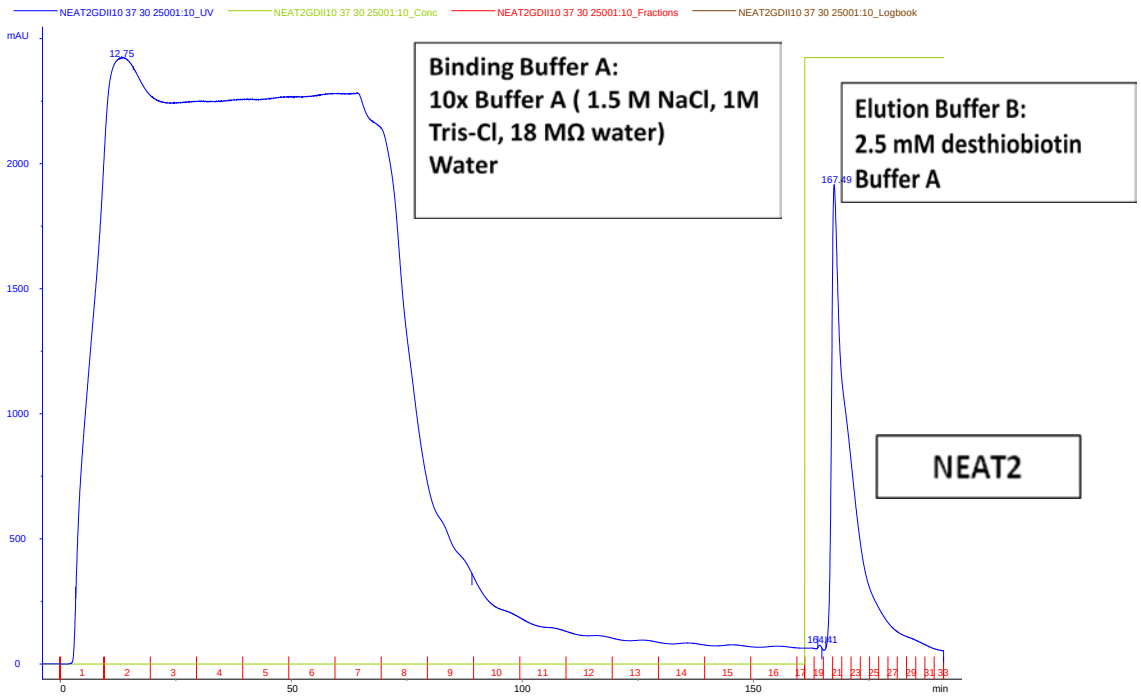

Figure 24. FPLC purification of NEAT2 grown in **Experiment IV** by stepwise method on a Strep Tactin Superflow high capacity column (IBA, St. Loius, MO, 5 mL). Buffers A and B were the binding and elution buffers, respectively. Fractions 20-32 were collected for centrifugation. Data taken at 280 nm.

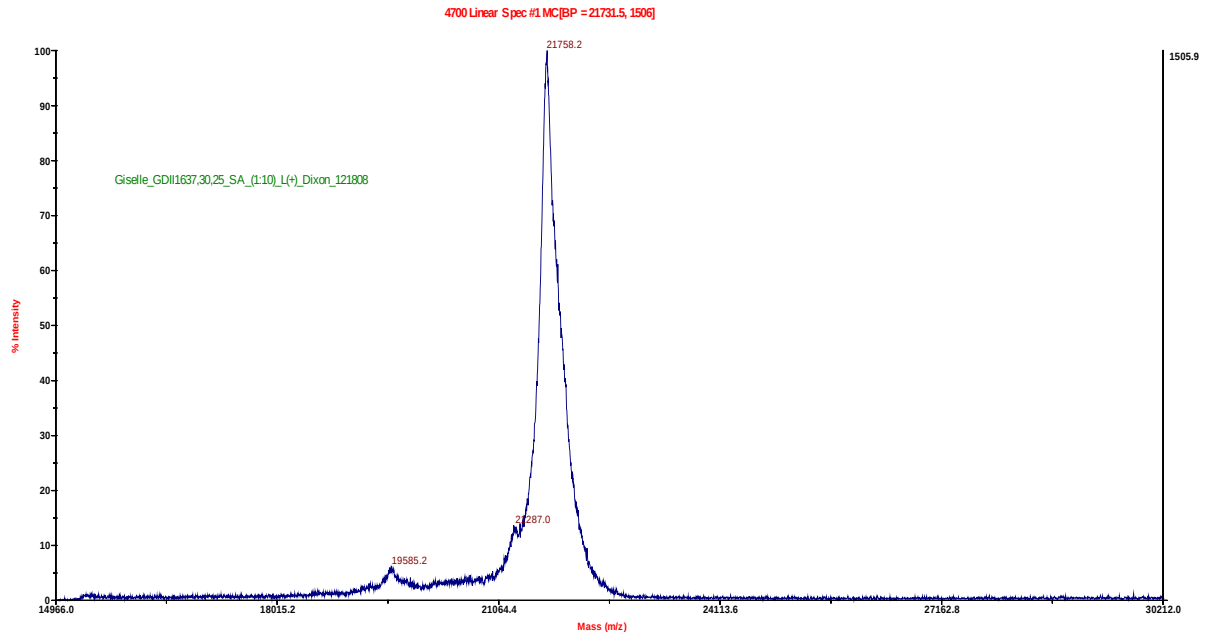

Figure 25. Mass spectrum of **Experiment IV**. The technique used was MALDI in the positive mode. The major peak was observed at 21758.2. The predicted mass for cleavage between Q and A in the sequence AQAAS is 21706.18. The experimental mass is within 0.2% of the predicted mass.

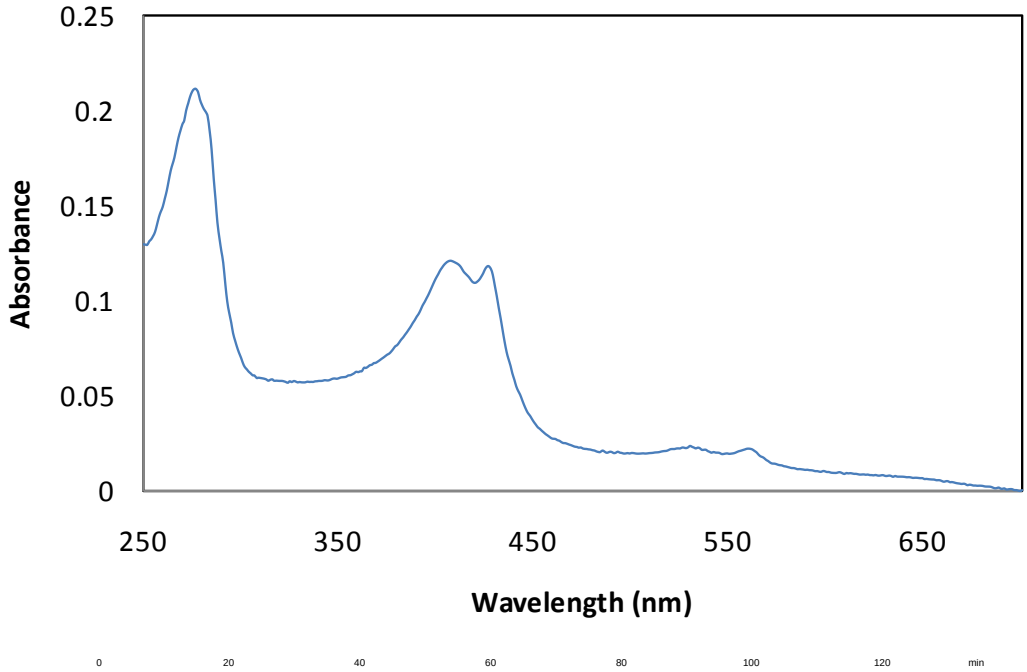

Figure 26. UV-visible spectrum of NEAT2 grown in **Experiment IV** after purification (20 mM Tris, pH 8.0). The 413 to 280 ratio is 0.613. The shoulder at 413 nm is presumed to be the Fe(III) form of the protein. The shoulder at 429 is presumed to be the Fe(II) of the protein. Maxima are also observed at 538 and 567 nm.

Binding Buffer A:
10x Buffer A (1.5 M NaCl, 1M Tris-Cl, 18 MΩ water)
Water

Elution Buffer B:
2.5 mM desthiobiotin
Buffer A

NEAT2

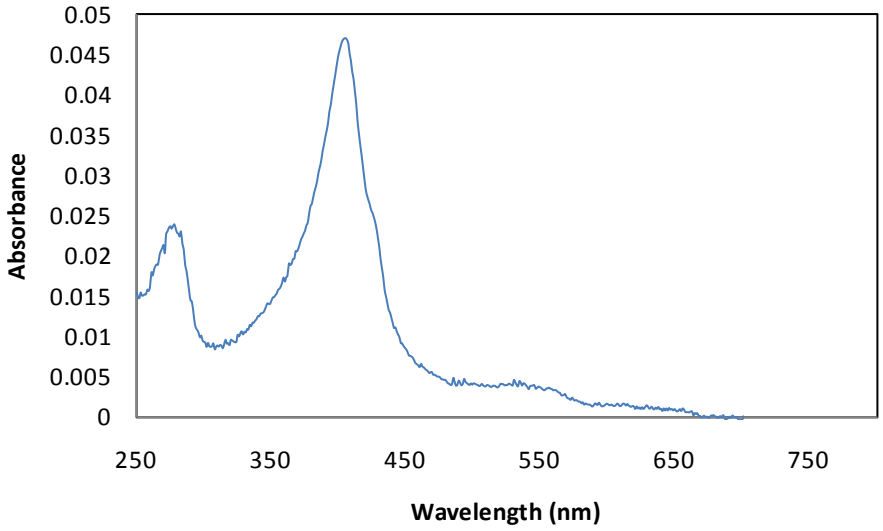

Figure 27. FPLC purification of NEAT2 grown in **Experiment V** by stepwise method on a Strep Tactin Superflow high capacity column (IBA, St. Loius, MO, 5 mL). Buffers A and B were the binding and elution buffers, respectively. Fractions 20-25 were collected for centrifugation. Data taken at 280 nm.

Figure 28. UV-visible spectrum of NEAT2 grown in **Experiment V** after purification in (20 mM Tris, pH 8.0). The 407 to 280 ratio is 2.28. The shoulder at 429 nm is presumed to be the Fe(II) form of the protein.

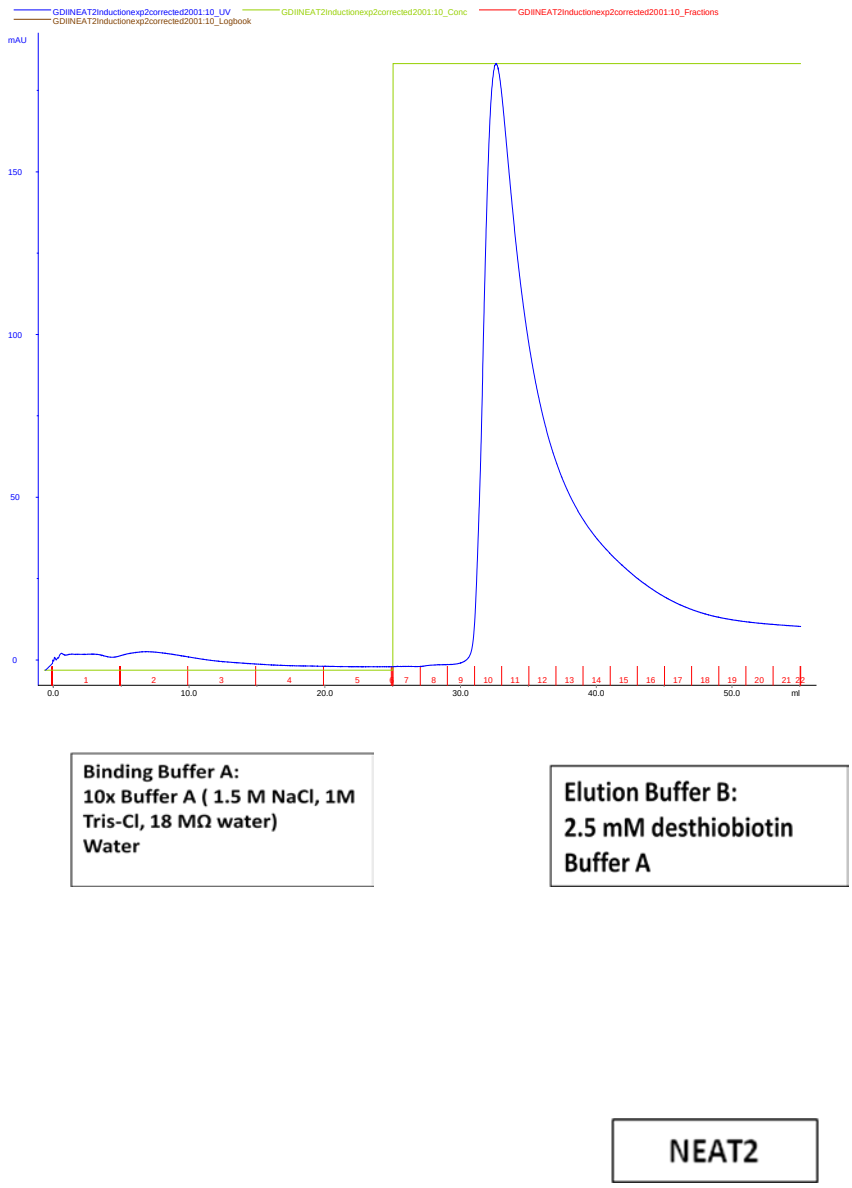

Figure 29. FPLC purification of NEAT2 grown in **Experiment B** by stepwise method on a Strep Tactin Superflow high capacity column (IBA, St. Loius, MO, 5 mL). Buffers A and B were the binding and elution buffers, respectively. Fractions 10-14 were collected for centrifugation. Data taken at 280 nm.

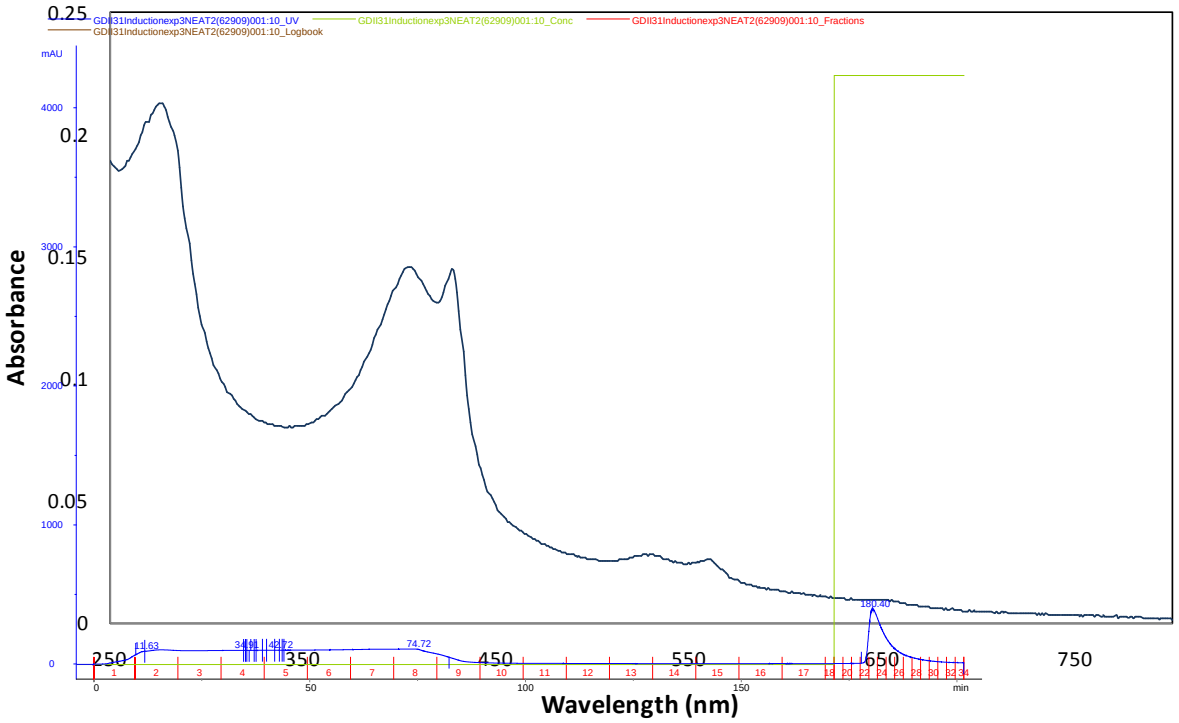

Figure 30. UV-visible spectrum of NEAT2 grown in **Experiment B** after purification (20 mM Tris, pH 8.0). The 404 to 280 ratio is 0.71. The shoulder at 426 nm is presumed to be the Fe (II) form of the protein. Maxima are also observed at 525, 555 and 651 nm.

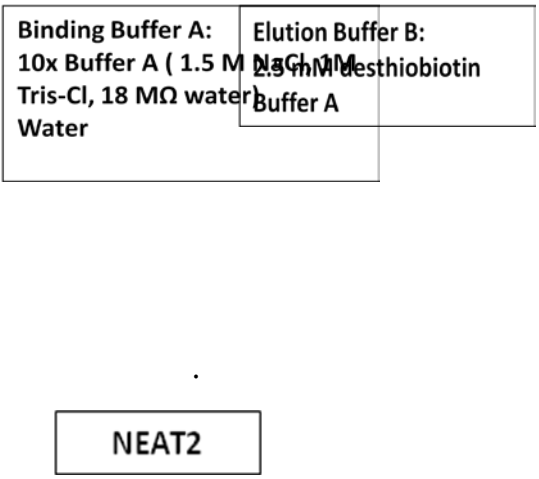

Figure 31. FPLC purification of NEAT2 grown in **Experiment C** by stepwise method on a Strep Tactin Superflow high capacity column (IBA, St. Loius, MO, 5 mL). Buffers A and B were the binding and elution buffers, respectively. Fractions 23-25 were collected for centrifugation. Data taken at 280 nm.

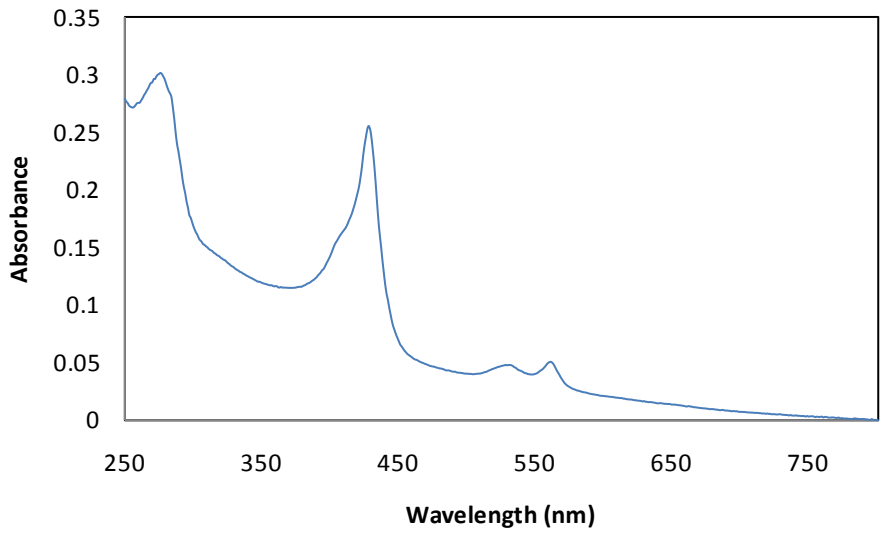

Figure 32. UV-visible spectrum of NEAT2 grown in **Experiment C** after purification (20 mM Tris, pH 8.0). The 427 to 273 ratio is 0.87. The shoulder at 406 nm is presumed to be the Fe (III) form of the protein. Maxima are also observed at 524 and 557 nm. Note that this protein was isolated largely in the reduced form.

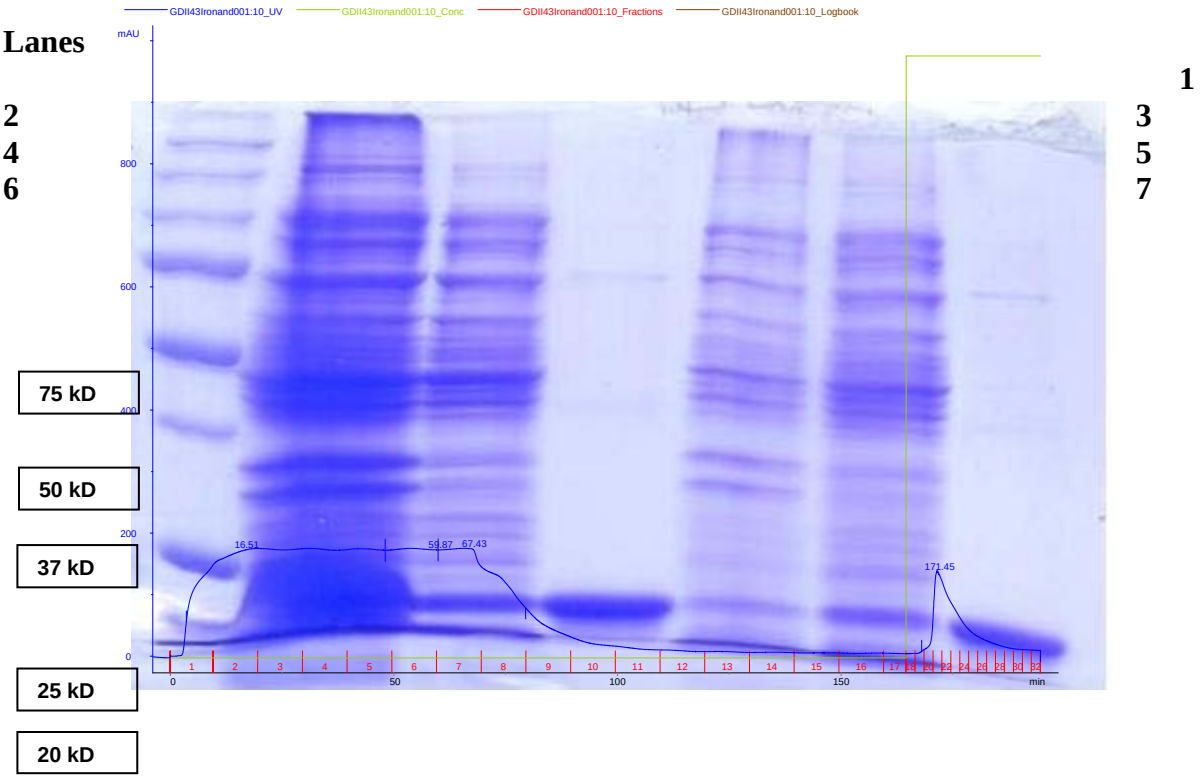

Figure 33. SDS-PAGE of NEAT2 grown with different **ALA** and **ALA plus Iron** concentrations. Lane 1: protein ladder. Lane 2 and 3: NEAT2 grown in Experiment ALA before (lane 2) and after (lane 3) French press. Lane 4: NEAT2 grown in Experiment ALA after purification. Lane 5 and 6: NEAT2 grown in Experiment ALA plus Iron before (lane 5) and after (lane 6) French press. Lane 7: NEAT2 grown n Experiment ALA plus Iron after purification.

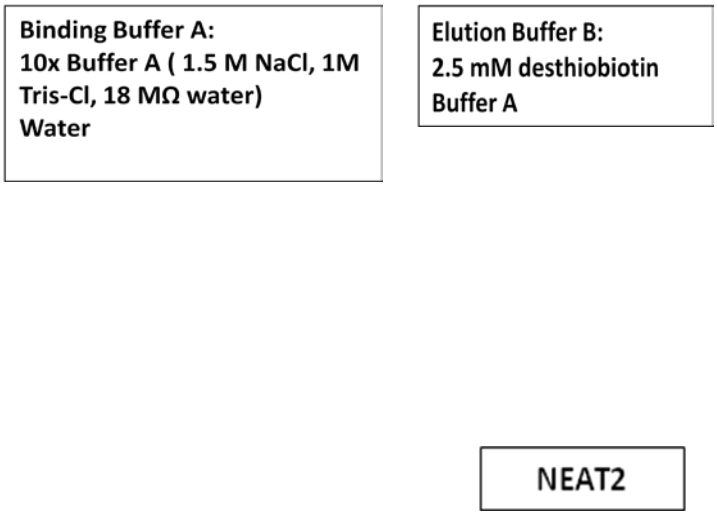

Figure 34. FPLC purification of NEAT2 grown in **Experiment ALA** by stepwise method on a Strep Tactin Superflow high capacity column (IBA, St. Loius, MO, 5 mL). Buffers A and B were the binding and elution buffers, respectively. Fractions 21-26 were collected for centrifugation. Data taken at 280 nm.

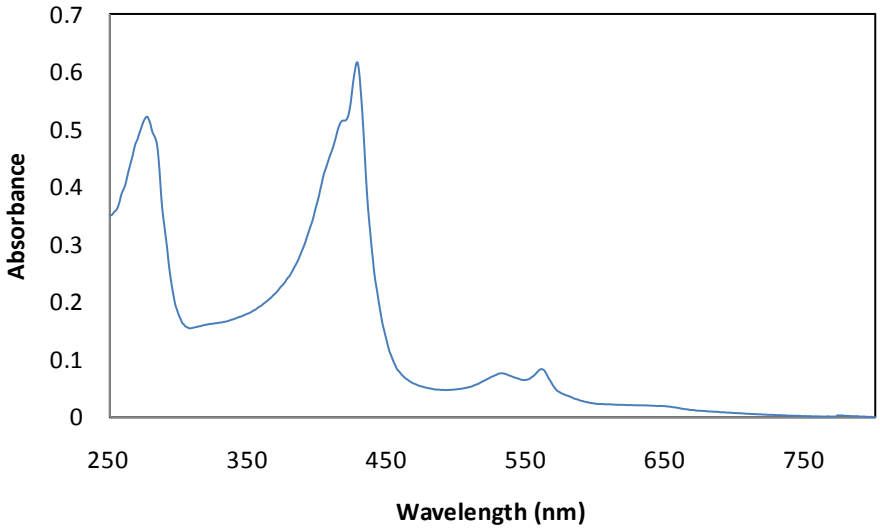

Figure 35. UV-visible spectrum of NEAT2 grown in **Experiment ALA** after purification (20 mM Tris, pH 8.0) fractions 21-23. The 428 to 280 ratio is 1.20. The shoulder at 419 nm is presumed to be the Fe(III) form of the protein. Maxima are also observed at 538, 564 and 656 nm.

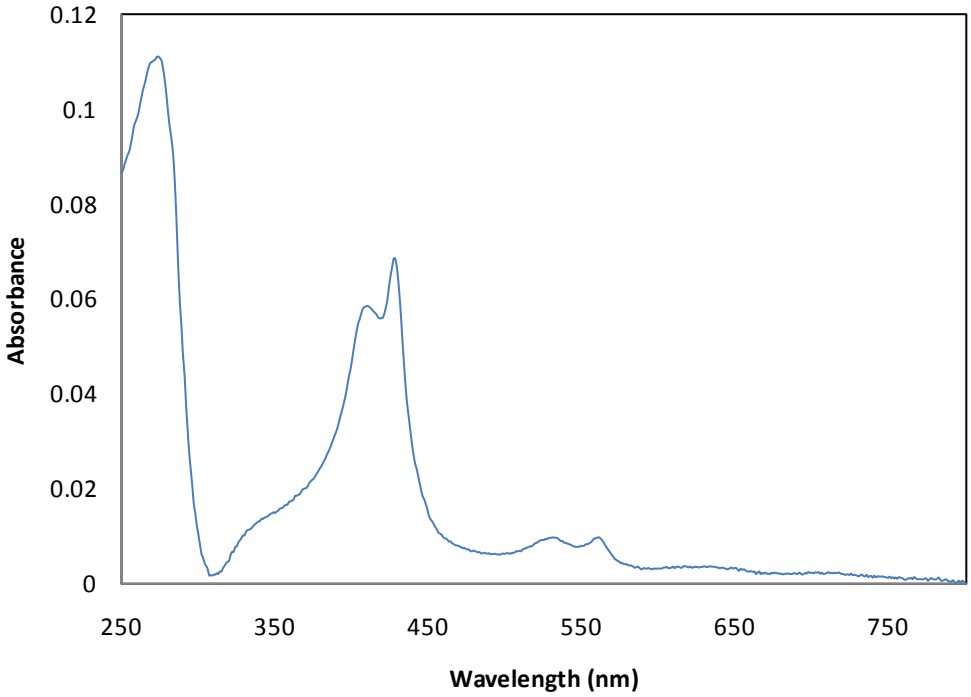

Figure 36. UV-visible spectrum of NEAT2 grown in **Experiment ALA Fractions 24-26** after purification (20 mM Tris, pH 8.0). The 429 to 276 ratio is 0.626. The shoulder at 414 nm is presumed to be the Fe(III) form of the protein. Maxima are also observed at 538 and 565 nm.

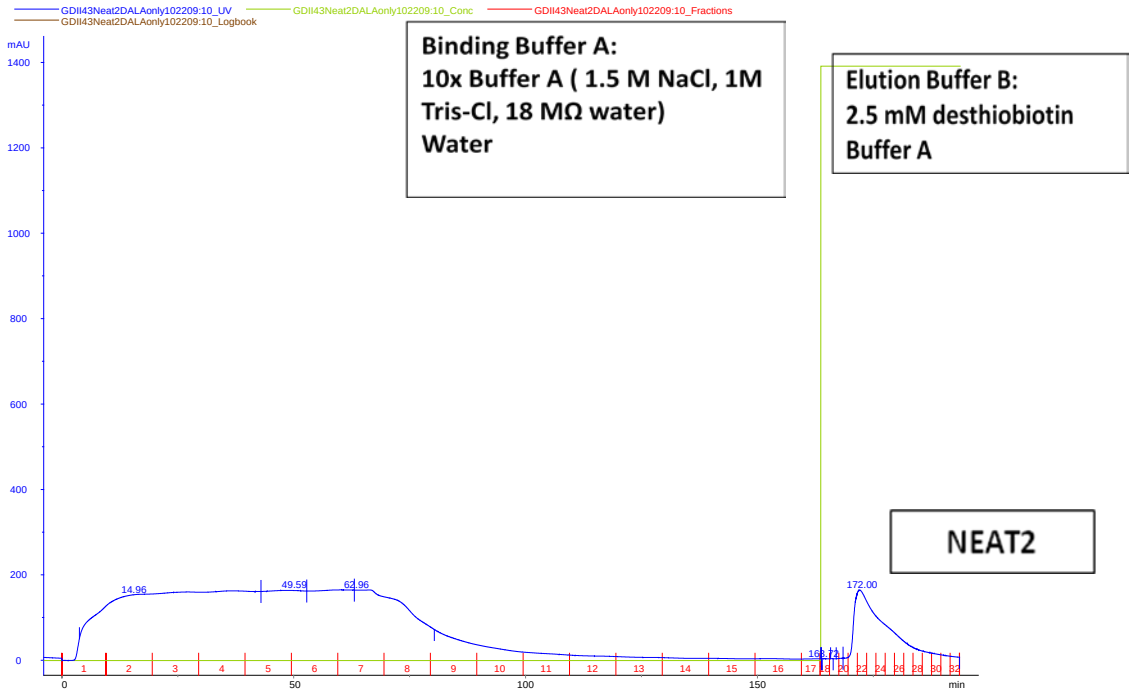

Figure 37. FPLC purification of NEAT2 grown in **Experiment ALA plus Iron** by stepwise method on a Strep Tactin Superflow high capacity column (IBA, St. Loius, MO, 5 mL). Buffers A and B were the binding and elution buffers, respectively. Fractions 21-25 were collected for centrifugation. Data taken at 280 nm.

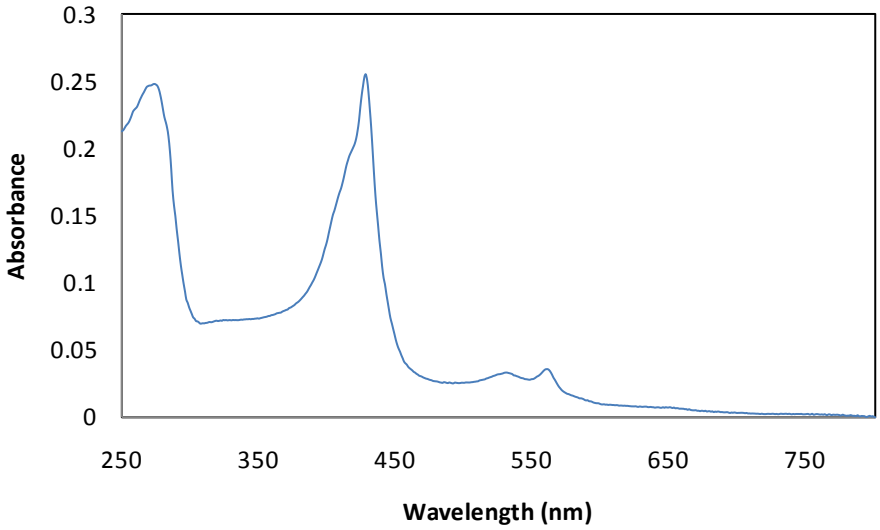

Figure 38. UV-visible spectrum of NEAT2 grown in **Experiment ALA and iron** after purification (20 mM Tris, pH 8.0). The 429 to 277 ratio is 1.03. The shoulder at 419 nm is presumed to be the Fe(III) form of the protein. Maxima are also observed at 535, 564 and 655 nm.

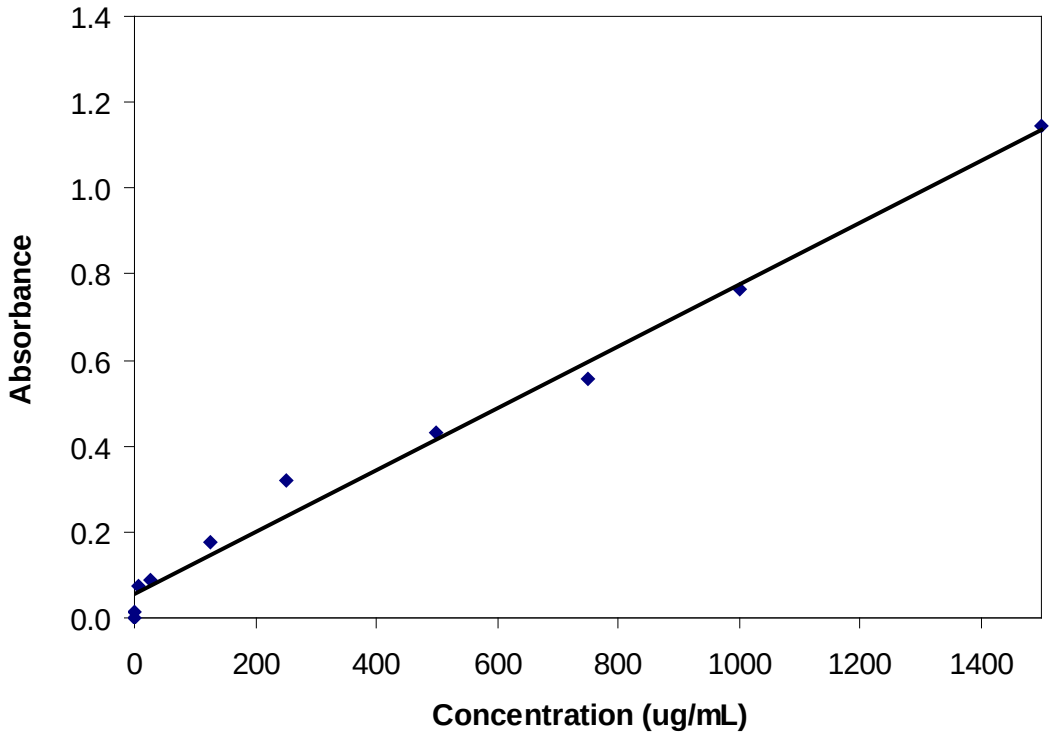

Figure 39. Lowry assay standard curve using a modified Lowry Protein Assay kit (Pierce, Rockford, IL). Diluted albumin (BSA) standards were prepared to construct a standard curve. Absorbance vs. concentration plot of known concentrations samples used to calculate unknown concentrations.

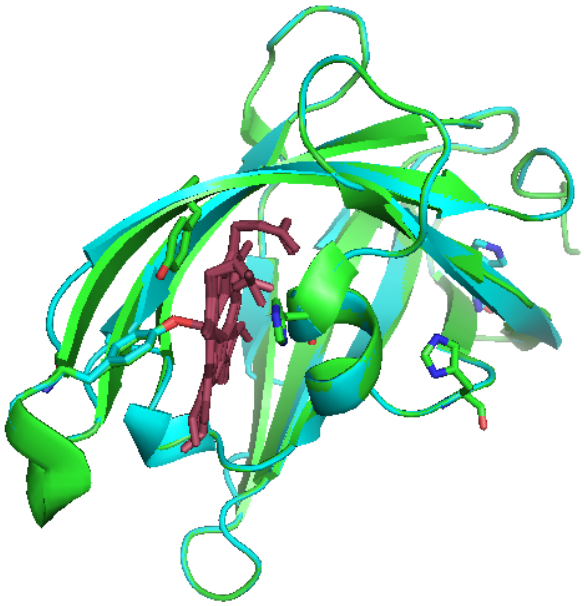

Figure 40. Shr-NEAT2 threaded into IsdA (2ITF.pdb). NEAT2 is green and IsdA is blue. Tyrosine is the axial ligand binding to heme (red). Helixes are indicated with ribbons and beta sheets are indicated with arrows. Figure created by PyMOL from the data in (Grigg et al., 2007b).

REFERENCE LIST

Altschul, S. F., Madden, T. L., Schaffer, A. A., Zhang, J., Zhang, Z., Miller, W., and Lipman, D. J. (1997). Gapped BLAST and PSI-BLAST: A new generation of protein database search programs. *Nucleic Acids Res.* **25**, 3389-3402.

Andrade, M. A., Ciccarelli, F. D., Perez-Iratxeta, C., and Bork, P. (2002). NEAT: A domain duplicated in genes near the components of a putative Fe(3+) siderophore transporter from Gram-positive pathogenic bacteria. *Genome Biol.* **3**, RESEARCH0047.

Aranda, R., Worley, C. E., Liu, M., Bitto, E., Cates, M. S., Olson, J. S., Lei, B. F., and Phillips, G. N. (2007). Bis-methionyl coordination in the crystal structure of the heme-binding domain of the streptococcal cell surface protein Shp. *J. Mol. Biol.* **374**, 374-383.

Austin, C. J. D., Mizdrak, J., Matin, A., Sirijovski, N., Kosim-Satyaputra, P., Willows, R. D., Roberts, T. H., Truscott, R. J. W., Polekhina, G., Parker, M. W., and Jamie, J. F. (2004). Optimised expression and purification of recombinant human indoleamine 2,3-dioxygenase. *Protein Expr. Purif.* **37**, 392-398.

Bates, C. S., Montañez, G. E., Woods, C. R., Vincent, R. M., and Eichenbaum, Z. (2003). Identification and characterization of a *Streptococcus pyogenes* operon involved in binding of hemoproteins and acquisition of iron. *Infect. Immun.* **71**, 1042-1055.

Borths, E. L., Locher, K. P., Lee, A. T., and Rees, D. C. (2002). The structure of *Escherichia coli* BtuF and binding to its cognate ATP binding cassette transporter. *Proc. Natl. Acad. Sci. USA* **99**, 16642-16647.

Cavallaro, G., Decaria, L., and Rosato, A. (2008). Genome-based analysis of heme biosynthesis and uptake in prokaryotic systems. *J. Proteome Res.* **7**, 4946-4954.

Clarke, S. R. and Foster, S. J. (2008). IsdA protects *Staphylococcus aureus* against the bactericidal protease activity of apolactoferrin. *Infect. Immun.* **76**, 1518-1526.

Clarke, T. E., Braun, V., Winkelmann, G., Tari, L. W., and Vogel, H. J. (2002). X-ray crystallographic structures of the *Escherichia coli* periplasmic protein FhuD bound to hydroxamate-type siderophores and the antibiotic albomycin. *J. Biol. Chem.* **277**, 13966-13972.

Crosa, J. H., Mey, A. R., and Payne, S. M. (2004). "Iron Transport in Bacteria." ASM Press, Washington, DC.

Cunningham, M. W. (2000). Pathogenesis of group A streptococcal infections. *Clin. Microbiol. Rev.* **13**, 470-511.

Dailey, H. A. (1997). Enzymes of heme biosynthesis. *J. Biol. Inorg. Chem.* **2**, 411-417.

Davidson, A. L. and Maloney, P. C. (2007). ABC transporters: how small machines do a big job. *Trends Microbiol.* **15**, 448-455.

DeLano, W. L. (2009). The PyMOL Molecular Graphics System. http://www.pymol.org.

Delcarte, J., Fauconnier, M. L., Jacques, P., Matsui, K., Thonart, P., and Marlier, M. (2003). Optimisation of expression and immobilized metal ion affinity chromatographic purification of recombinant (HiS)(6)-tagged cytochrome P450 hydroperoxide lyase in *Escherichia coli*. *J. Chrom. B - Anal. Tech. Biomed. Life Sci.* **786**, 229-236.

Eakanunkul, S., Lukat-Rodgers, G. S., Sumithran, S., Ghosh, A., Rodgers, K. R., Dawson, J. H., and Wilks, A. (2005). Characterization of the periplasmic heme-binding protein ShuT from the heme uptake system of *Shigella dysenteriae*. *Biochemistry* **44**, 13179-13191.

Eichenbaum, Z., Muller, E., Morse, S. A., and Scott, J. R. (1996). Acquisition of iron from host proteins by the group A *Streptococcus*. *Infect. Immun.* **64**, 5428-5429.

Finn, R. D., Tate, J., Mistry, J., Coggill, P. C., Sammut, S. J., Hotz, H. R., Ceric, G., Forslund, K., Eddy, S. R., Sonnhammer, E. L. L., and Bateman, A. (2008). The Pfam protein families database. *Nucleic Acids Res.* **36**, D281-D288.

Francis, R. T., Jr., Booth, J. W., and Becker, R. R. (1985). Uptake of iron from hemoglobin and the haptoglobin-hemoglobin complex by hemolytic bacteria. *Int. J. Biochem.* **17**, 767-773.

Gasteiger, E., Hoogland, C., Gattiker, A., Duvaud, S., Wilkins, M. R., Appel, R. D., and Bairoch, A. (2005). Protein identification and analysis tools on the ExPASy server. *In* "The Proteomics Protocols Handbook" (J. M. Walker, Ed.), pp. 571-607. Humana Press, Totowa, N.J.

Grigg, J. C., Vermeiren, C. L., Heinrichs, D. E., and Murphy, M. E. (2007a). Heme coordination by *Staphylococcus aureus* IsdE. *J. Biol. Chem.* **282**, 22815-28822.

Grigg, J. C., Vermeiren, C. L., Heinrichs, D. E., and Murphy, M. E. P. (2007b). Haem recognition by a *Staphylococcus aureus* NEAT domain. *Mol. Microbiol.* **63**, 139-149.

Heinemann, I. U., Jahn, M., and Jahn, D. (2008). The biochemistry of heme biosynthesis. *Arch. Biochem. Biophys.* **474**, 238-251.

Hollenstein, K., Dawson, R. J. P., and Locher, K. P. (2007). Structure and mechanism of ABC transporter proteins. *Curr. Opin. Struct. Biol.* **17**, 412-418.

Jones, P. M. and George, A. M. (2004). The ABC transporter structure and mechanism: Perspectives on recent research. *Cell Mol. Life Sci.* **61**, 682-699.

Krewulak, K. D. and Vogel, H. J. (2008). Structural biology of bacterial iron uptake. *Biochim. Biophys. Acta Biomembranes* **1778**, 1781-1804.

Kumar, A. and Schweizer, H. P. (2005). Bacterial resistance to antibiotics: Active efflux and reduced uptake. *Advanced Drug Delivery Reviews* **57**, 1486-1513.

Lei, B. F., Liu, M. Y., Prater, C. I., Kala, S. V., Deleo, F. R., and Musser, J. M. (2003). Identification and characterization of HtsA, a second heme-binding protein made by *Streptococcus pyogenes*. *Infect. Immun.* **71**, 5962-5969.

Lei, B. F., Smoot, L. M., Menning, H. M., Voyich, J. M., Kala, S. V., Deleo, F. R., Reid, S. D., and Musser, J. M. (2002). Identification and characterization of a novel heme-associated cell surface protein made by *Streptococcus pyogenes*. *Infect. Immun.* **70**, 4494-4500.

Li, X. Z. and Nikaido, H. (2009). Efflux-mediated drug resistance in bacteria: An update. *Drugs* **69**, 1555-1623.

Liu, M. Y. and Lei, B. F. (2005). Heme transfer from streptococcal cell surface protein Shp to HtsA of transporter HtsABC. *Infect. Immun.* **73**, 5086-5092.

Martinez, J. L., Sanchez, M. B., Martinez-Solano, L., Hernandez, A., Garmendia, L., Fajardo, A., and Alvarez-Ortega, C. (2009). Functional role of bacterial multidrug efflux pumps in microbial natural ecosystems. *FEMS Microbiol. Rev.* **33**, 430-449.

Muller, A., Wilkinson, A. J., Wilson, K. S., and Duhme-Klair, A. K. (2006). An [{Fe(mecam)}$(_2)$]$(^{6-})$ bridge in the crystal structure of a ferric enterobactin binding protein. *Angew. Chem. Int. Ed.* **45**, 5132-5136.

Muryoi, N., Tiedemann, M. T., Pluym, M., Cheung, J., Heinrichs, D. E., and Stillman, M. J. (2008). Demonstration of the iron-regulated surface determinant (Isd) heme transfer pathway in *Staphylococcus aureus*. *J. Biol. Chem.* **283**, 28125-28136.

Nygaard, T. K., Blouin, G. C., Liu, M. Y., Fukumura, M., Olson, J. S., Fabian, M., Dooley, D. M., and Lei, B. F. (2006). The mechanism of direct heme transfer from the streptococcal cell surface protein Shp to HtsA of the HtsABC transporter. *J. Biol. Chem.* **281**, 20761-20771.

Olczak, T. (2006). Analysis of conserved glutamate residues in Porphyromonas gingivalis outer membrane receptor HmuR: toward a further understanding of heme uptake. *Arch. Microbiol.* **186**, 393-402.

Olczak, T., Sroka, A., Potempa, J., and Olczak, M. (2008). *Porphyromonas gingivalis* HmuY and HmuR: Further characterization of a novel mechanism of heme utilization. *Arch. Microbiol.* **189**, 197-210.

Pilpa, R. M., Robson, S. A., Villareal, V. A., Wong, M. L., Phillips, M., and Clubb, R. T. (2009). Functionally distinct NEAT (NEAr Transporter) domains within the *Staphylococcus aureus* IsdH/HarA protein extract heme from methemoglobin. *J. Biol. Chem.* **284**, 1166-1176.

Pishchany, G., Dickey, S. E., and Skaar, E. P. (2009). Subcellular localization of the *Staphylococcus aureus* heme iron transport components IsdA and IsdB. *Infect. Immun.* **77**, 2624-2634.

Pluym, M., Muryol, N., Heinrichs, D. E., and Stillman, M. J. (2008). Heme binding in the NEAT domains of IsdA and IsdC of *Staphylococcus aureus*. *J. Inorg. Biochem.* **102**, 480-488.

Pluym, M., Vermeiren, C. L., Mack, J., Heinrichs, D. E., and Stillman, M. J. (2007). Heme binding properties of *Staphylococcus aureus* lsdE. *Biochemistry* **46**, 12777-12787.

Poole, K. (2007). Efflux pumps as antimicrobial resistance mechanisms. *Ann. Med.* **39**, 162-176.

Sayle, R. A. and Milner-White, E. J. (1995). Rasmol - Biomolecular graphics for all. *Trends in Biochemical Sciences* **20**, 374-376.

Sharp, K. H., Schneider, S., Cockayne, A., and Paoli, M. (2007). Crystal structure of the heme-IsdC complex, the central conduit of the isd iron/heme uptake system in *Staphylococcus aureus*. *J. Biol. Chem.* **282**, 10625-10631.

Skaar, E. P. and Schneewind, O. (2004). Iron-regulated surface determinants (Isd) of *Staphylococcus aureus*: Stealing iron from heme. *Microbes Infect.* **6**, 390-397.

Sook, B. R., Block, D. R., Sumithran, S., Montañez, G. E., Rodgers, K. R., Dawson, J. H., Eichenbaum, Z., and Dixon, D. W. (2008). Characterization of SiaA, a streptococcal heme-binding protein associated with a heme ABC transport system. *Biochemistry* **47**, 2678-2688.

Suits, M. D. L., Lang, J., Pal, G. P., Couture, M., and Jia, Z. C. (2009). Structure and heme binding properties of *Escherichia coli* O157:H7 ChuX. *Protein Sci.* **18**, 825-838.

Teodorescu, O., Galor, T., Pillardy, J., and Elber, R. (2004). Enriching the sequence substitution matrix by structural information. *Proteins-Structure Function and Bioinformatics* **54**, 41-48.

Tong, Y. and Guo, M. (2009). Bacterial heme-transport proteins and their heme-coordination modes. *Arch. Biochem. Biophys.* **481**, 1-15.

Tong, Y. and Guo, M. L. (2007). Cloning and characterization of a novel periplasmic heme-transport protein from the human pathogen *Pseudomonas aeruginosa*. *J. Biol. Inorg. Chem.* **12**, 735-750.

Torres, V. J., Pishchany, G., Humayun, M., Schneewind, O., and Skaar, E. P. (2006). *Staphylococcus aureus* IsdB is a hemoglobin receptor required for heme iron utilization. *J. Bacteriol.* **188**, 8421-8429.

Villareal, V. A., Pilpa, R. M., Robson, S. A., Fadeev, E. A., and Clubb, R. T. (2008). The IsdC protein from *Staphylococcus aureus* uses a flexible binding pocket to capture heme. *J. Biol. Chem.* **283**, 31591-31600.

Wandersman, C. and Delepelaire, P. (2004). Bacterial iron sources: From siderophores to hemophores. *Annu. Rev. Microbiol.* **58**, 611-647.

Watanabe, M., Tanaka, Y., Suenaga, A., Kuroda, M., Yao, M., Watanabe, N., Arisaka, F., Ohta, T., Tanaka, I., and Tsumoto, K. (2008). Structural basis for multimeric heme complexation through a specific protein-heme interaction - The case of the third NEAT domain of IsdH from *Staphylococcus aureus*. *J. Biol. Chem.* **283**, 28649-28659.

Wilks, A. and Burkhard, K. A. (2007). Heme and virulence: How bacterial pathogens regulate, transport and utilize heme. *Nat. Prod. Reports* **24**, 511-522.

Wojtowicz, H., Guevara, T., Tallant, C., Olczak, M., Sroka, A., Potempa, J., Sola, M., Olczak, T., and Gomis-Ruth, F. X. (2009a). Unique structure and stability of HmuY, a novel heme-binding protein of *Porphyromonas gingivalis*. *PLoS Pathogens* **5**.

Wojtowicz, H., Olczak, M., and Olczak, T. (2009b). Investigation of heme transport by *Porphyromonas gingivalis* HmuY protein through the stability studies. *FEBS J.* **276**, 171-172.

Wojtowicz, H., Wojaczynski, J., Olczak, M., Kroliczewski, J., Latos-Grazynski, L., and Olczak, T. (2009c). Heme environment in HmuY, the heme-binding protein of *Porphyromonas gingivalis*. *Biochem. Biophys. Res. Commun.* **383**, 178-182.

Zhu, H., Liu, M. Y., and Lei, B. F. (2008a). The surface protein Shr of *Streptococcus pyogenes* binds heme and transfers it to the streptococcal heme-binding protein Shp. *BMC Microbiology* **8**.

Zhu, H., Xie, G., Liu, M. Y., Olson, J. S., Fabian, M., Dooley, D. M., and Lei, B. F. (2008b). Pathway for heme uptake from human methemoglobin by the iron-regulated surface determinants system of *Staphylococcus aureus*. *J. Biol. Chem.* **283**, 18450-18460.